FUNDAMENTALS OF THE DOUBLE-HUMPED FISSION BARRIER

M. BRACK
Institut Laue-Langevin,
Grenoble, France

ABSTRACT

We review the development of the theory of the fission barrier over the past forty years. Special emphasis is put on the shell-correction method of Strutinsky and its foundation and numerical verification from microscopical Hartree-Fock calculations. The different practical realisations of the method and its applications to the calculation of deformation energy surfaces are reviewed. The influence of the different shape degrees of freedom of the nucleus on the form of the fission barrier is discussed. Finally, we summarize some more recent developments concerning both experimental and theoretical aspects of the double-humped fission barrier.

INTRODUCTION

These notes cover the contents of six lectures presented at the Winter Course on Nuclear Theory for Applications, held at the ICTP in 1978.

Almost all of what was discussed in the lectures has been published before extensively; we shall therefore not repeat here details of mathematical derivations or numerical computations. For these, we refer to the literature. The main purpose of these notes is to give the reader an introduction to the different physical models which are employed in the theory of the fission barrier. With the help of illustrative examples, we shall summarize the results of different calculations and give an impression of their reliability and their agreement with experimental results.

1. HISTORICAL REVIEW OF THE FISSION BARRIER

1.1. Discovery of Fission

A nice historical account of the discovery of fission is given in the book of Hyde, 1964, p.3 (with detailed references). Fermi and collaborators in Rome (1934/5)[1] bombarded uranium (Z = 92) with paraffin-slowed neutrons. They tried to explain the resulting radioactivity as coming from a new element (Z = 93) or even several "transuranium" elements. However, too many activities were seen and the radiochemical properties were too unexpected to be explained in this way. The situation remained confused, until in 1939, Hahn and Strassmann [2] and Meitner and Frisch[3] recognized the new process as the fissioning of the nucleus into (normally two) fragments.

Immediately after the discovery of fission, Meitner and Frisch[3] also gave a qualitative theoretical explanation of the process using the analogy of a charged liquid drop. Still in the same year, 1939, two independent theoretical papers appeared, using and developing the same basic picture: a short one of Fraenkel [Fr39], and an extensive one of Bohr and Wheeler [BW39], which became and remained a classic for many years to come.

1.2. The liquid drop model

This model uses an idealization of the nucleus as a uniformly charged liquid drop. The attractive nuclear forces are summarized by a (classical) surface tension. The stability or decay (fissioning) of the nucleus is governed by the interplay between this attractive surface tension and the repulsive Coulomb force.

This same model underlies the semi-empirical mass formula developed by Weizsäcker[We35] and Bethe[BB36,Be37] (see also [BK37]), in which the total mass (binding energy) of a nucleus is written in the form

[1] E. Fermi, Nature 133 (1934) 898; E. Amaldi et al. Proc. Roy. Soc. A149 (1935) 522.
[2] O. Hahn and F. Strassmann , Naturwiss. 27 (1939), p.11 and p.89.
[3] L. Meitner and O.R. Frisch, Nature 143 (1939) p.239 and p.471

$$E(N,Z) = a_v(1+\kappa_v I^2)A + a_s(1+\kappa_s I^2)A^{2/3} + \dots$$
$$+ C_d Z(Z-1)A^{-1/3} + C_{ex} Z^{4/3} A^{-1} + \dots \qquad (1.1)$$
$$+ P(N,Z) + \delta E(N,Z)$$

with

$$A = N+Z \ , \quad I = \left(\frac{N-Z}{A}\right).$$

Here a_v and a_s are the so-called volume and surface energies, κ_v and κ_s the asymmetry coefficients, the terms with C_d and C_{ex} are the direct and exchange Coulomb energies, P(N,Z) is a (relatively small) pairing energy ($\sim \pm 2$ MeV) and δE the so-called shell-correction energy. All terms but δE are smooth functions of N and Z and constitute the main part ($\gtrsim$ 99% in a heavy nucleus) of the binding energy. We express this by writing (1.1) in the form

$$E(N,Z) = E_{LDM}(N,Z) + \delta E(N,Z). \qquad (1.2)$$

The LDM accounts for all terms included in E_{LDM} (except for P(N,Z) which we include for convenience).

In the application of this model to the fission process, one is interested in the deformation energy, i.e. the difference $E^{def}_{LDM}(\beta)$ between the energy at a given deformation (we summarize all possible deformation parameters by β) minus that of the spherical shape $\beta = 0$. To this difference, only the surface and Coulomb terms contribute in E_{LDM}; the volume term falls out due to the fact that nuclear matter is (almost) incompressible. The deformation energy is thus written as the sum of a surface and a Coulomb energy:

$$E^{def}_{LDM}(\beta) = E_{Surf}(\beta) + E_{Coul}(\beta) \tag{1.3}$$

(both normalized to zero at $\beta = 0$, i.e. spherical shape).

We come back to the parametrization of the nuclear shape (i.e. the exact meaning of β) in lesson 4.

In his book on "Theories of Nuclear Fission", 1964, Wilets presents the LDM and results of deformation energy calculations very extensively, summarizing both the original papers[BW39, Fr39] and later extensions, the last of which [CS63] containing large-scale numerical computer calculations. Not mentioned there is another important paper [SL63].

The critical parameter in the LDM is the so-called "fissionability" (or fissility) parameter X, defined as the ratio of the Coulomb energy and twice the surface energy of a charged sphere with radius R_0:

$$X = E_{Coul}(0) / 2E_{Surf}(0) \tag{1.4}$$

with

$$E_{Coul}(0) = \tfrac{3}{5} \cdot Z^2 e^2 / R_0 \; ; \quad E_{Surf}(0) = 4\pi R_0^2 \tau . \tag{1.5}$$

Here τ is the surface tension. Using the experimentally known A-dependence of the nuclear radius

$$R_0 = r_0 A^{1/3} \quad , \quad r_0 \simeq 1.2 \text{ fm} , \tag{1.6}$$

we can relate τ to the surface term in the mass formula (1.1):

$$\tau = a_s (1 + \kappa_s I^2) / 4\pi r_0^2 . \tag{1.7}$$

Combining eqs.(1.5)-(1.7) we see that the fissility parameter X, apart from the relatively weak I^2-dependence of τ , goes like Z^2/A. One therefore frequently puts

$$X = (Z^2/A) / (Z^2/A)_{crit} . \tag{1.8}$$

With the above constants and the empirical values $a_s \simeq 18$ MeV, $\kappa_s \simeq -2.5$, one obtains

$$(Z^2/A)_{crit} \approx 45 - 50 . \tag{1.9}$$

In most early LDM calculations, one used the multipole expansion of the deformed nuclear surface [BW39]:

$$R(\vartheta,\varphi) = R_0 \left[1 + \sum_{\lambda,\mu} a_{\lambda\mu} Y_{\lambda\mu}(\vartheta,\varphi) \right] . \tag{1.10}$$

The $\{a_{\lambda\mu}\}$ thus represent one possible set of deformation parameters β.

Main results of LDM calculations:

1) For $X < 1$, the spherical configuration (all $a_{\lambda\mu} = 0$) is a stable local minimum. Thus, the LDM predicts spherical groundstates for all stable nuclei. For $X > 1$, the spherical shape becomes unstable against quadrupole (a_{20}) deformation, the nucleus then is spontaneously deforming itself until it fissions. Thus, the LDM predicts spontaneous fission for all nuclei with $X > 1$. (N.B. A heavy actinide nucleus has $X \simeq 0.8$, i.e. $(Z^2/A) \simeq 40$).

2) For $0.7 \lesssim X < 1$ the deformation energy surface, $E^{def}_{LDM}(a_{\lambda\mu})$ has a saddle point with positive energy E_f relative to the ground state. This result is qualitatively already found if only a_{20} and a_{40} deformations are used, see Fig. 1.1. The saddle point has always positive (prolate) quadrupole deformation. Along a static path over the saddle point (way of steepest descent), one obtains thus a fission barrier with height E_f. Numerical calculations including multipoles up to $\lambda \simeq 16$ in eq.(1.10) lead to [CS63]

$$E_f \approx 0.83 E_{Surf}(0) (1-X)^3 , \qquad 0.67 < X < 1 . \tag{1.11}$$

In Table 1.1 we show a comparison of the calculated values of E_f with the experimental barriers measured up to $\sim$ 1960 (assuming a single-humped form of the barrier). The agreement is bad. Whereas E_f^{LDM} varies from $\sim$ 15 to $\sim$9 MeV, the experimental barriers are all around $\sim$ 5.5 to 6.5 MeV. The LDM thus gives the wrong quantitative behaviour of the barrier heights.

3) For $X > 0.39$, the deformation energy is always stable against rotationally asymmetric ($\mu \neq 0$) and reflection (left/right) asymmetric (λ odd) deformations. In other words, only the parameters $a_{\lambda 0}$ with λ even are different from zero. As a consequence, the LDM cannot explain the asymmetric mass split in fission.

The main failures of the LDM (no static deformations, wrong fission barriers, no asymmetric fission) are due to the missing of quantum mechanical effects (shell effects). As a hint we may take the order of magnitude of the empirical shell-corrections δE to the goundstate masses [MS66]:

$$|\delta E| \approx |\delta M| \simeq 5 - 15 \text{ MeV}. \tag{1.12}$$

This is very small compared to the total binding energies of heavy nuclei ($\sim$ 1000 - 2000 MeV), but it becomes important when compared to the heights of the fission barriers E_f!

The LDM provides thus a nice qualitative description of the fission process, but for a quantitative theory the shell effects have to be included.

1.3 The (deformed) shell model

The shell model [HJ49, Ma49] emphasizes the quantum mechanical structure of the nucleus as a system of Z protons and N neutrons. The mutual nuclear interaction between the neutrons (protons) is summarized by an average potential $V_n(V_p)$ in which the particles are assumed to move independently. For each kind (n or p), a Schrödinger equation is solved

$$\left[-\frac{\hbar^2}{2m}\Delta + V(\underline{r})\right]\varphi_i(\underline{r}) = \varepsilon_i\,\varphi_i(\underline{r}) \tag{1.13}$$

to obtain the levels ε_i and wavefunctions of the individual nucleons. In the g.-s., the lowest N(Z) states are filled. The potentials $V_n(\underline{r})$ and $V_p(\underline{r})$ contain a local (central) and a spin-orbit part. $V_p(\underline{r})$ includes also a Coulomb potential.

In connection with fission, we are mostly interested in the extension of the shell model to deformed nuclei, which was introduced by Nilsson [Ni55]. In the Nilsson model, the potentials V_n and V_p are deformed along with the shape of the nucleus. The solutions of the Schrödinger equation (1.13) then depend also on the deformation parameters; this gives the familiar Nilsson level schemes, see Fig. 1.2.

In the independent particle model, the total energy is

$$E(\beta) = \sum_{i=1}^{N}\varepsilon_i^n(\beta) + \sum_{i=1}^{Z}\varepsilon_i^p(\beta). \tag{1.14}$$

Strictly, the justification of the shell model is given in Hartree-Fock theory, where eq.(1.14) is not equal to the total binding energy (see lesson 2). However, for harmonic oscillator potentials (and thus also approximately for the Nilsson model), the total energy is still proportional to (1.14).

A comprehensive description of the Nilsson model is given in the book of Preston and Bhaduri.

Minimisation of the energy E(β) (1.14) with respect to β leads to the groundstate deformation β_o. Good agreement with the experimental deformations of rare earth and actinide nuclei is obtained[1,2]. From the Nilsson spectra $\varepsilon_i(\beta_o)$ at the groundstate, other properties such as spin, magnetic moment and single particle spectra of odd-A nuclei can be derived.

When extended to large deformations, the model fails. The deformation energy (1.14) was found to increase too steeply and not to lead to any reasonable fission barrier[3] (see also [NT69]). Similar results were also found in the two-center shell model (e.g.[SG71]).

The reason for this breakdown is the lack of self-consistency of the used average deformed potentials and of the expression (1.14) for the total energy. At small (groundstate) deformations, the experimental spectroscopic information allows to parametrize the shell model potentials sufficiently well. But when extrapolating to large deformations, the results depend very crucially on the parameters and on the way in which the potentials are deformed.

Myers and Swiatecki [MS66] discussed the connection between the non-uniformities of the shell model spectra ε_i and the magnitude of the empirical shell corrections δE in (1.1). Large gaps in the spectrum ("magic" nucleon numbers) lead to increased binding (negative δE). This is not only restricted to spherical nuclei [St66,67]; deformed shells exist as well (Fig. 1.2)

The first quantitative prescription to calculate δE from the spectrum ε_i was given by Strutinsky [St66-68].

1.4 The shell-correction method (SCM) ("Strutinsky method")

Strutinsky defines the shell-correction δE for each kind of particles by

$$\delta E_{p(n)} = \sum_{i=1}^{Z(N)}\varepsilon_i^{p(n)} - \tilde{E}_{p(n)}, \tag{1.15}$$

i.e. the difference between the sum of occupied levels and its average part

$$\tilde{E}_{p(n)} = \left\langle \sum_{i=1}^{Z(N)}\varepsilon_i^{p(n)} \right\rangle. \tag{1.16}$$

(The precise definition of the average energies $\tilde{E}_{p(n)}$ will be given in lesson 4). The total energy of the nucleus is then the LDM energy plus the shell-corrections:

$$E(N,Z,\beta) = E_{LDM}(N,Z,\beta) + \delta E_p(Z,\beta) + \delta E_n(N,\beta). \tag{1.17}$$

This means a renormalization of the average parts of the single-particle energies by the LDM energy. One is thus combining the correct average energy of the LDM with the (at least at small deformations) correct fluctuating part δE of the shell model energy (1.14).

[1] B. Mottelson and S.G. Nilsson, Kgl. Dan. Vid. Selsk. Mat. Fys. Skr. 1, no.8 (1955)
[2] D. Bès and Z. Szymanski, Nucl. Phys. 28 (1961) 42.
[3] S.A.E. Johansson, Nucl. Phys. 22 (1962) 529.

The theoretical quantitative justification of eq.(1.17) can be given in the Hartree-Fock theory and will be discussed in lesson 3.

Main Results of SCM calculations: (Details see lessons 4-6)

1) Explanation of the fission isomers, which had been known long ago [Po62] but not understood, in terms of a double-humped fission barrier which turns out for most actinide nuclei.

2) Quantitative agreement between theoretical and experimental barrier heights; usually within ∿ 1-2 MeV (except for neutron-poor lighter actinides; so-called "Th-anomaly").

3) Ground-state deformations in excellent agreement with experimental ones. The g.s. mass corrections δE(δM) agree with the empirical ones within ∿1-2 MeV (except sometimes in the Pb^{208} region; so-called "Pb-anomaly").

4) Qualitative explanation of mass asymmetry of the fission products due to shell effects, both at the outer saddle point and at the scission point (see lesson 6).

5) Prediction of a possible island (or several) of stable nuclei with $Z \sim 114$-126 or larger; "superheavy nuclei"?

In summary, the Strutinsky method brought a break-through in the theory of the fission barrier, allowing for the first time a quantitatively satisfactory calculation of barrier heights and giving the explanation of the fission isomers as shape isomers. In this method, both the LDM and the shell model are given their balanced role.

1.5 The Hartree-Fock method (HF)

The HF method allows to calculate nuclear properties starting from an effective nucleon-nucleon interaction $V_{eff}(r_1-r_2)$. This is a basically microscopic, quantum mechanical theory, in which only the parameters of the interaction V_{eff} are adjustable. The HF method is the subject of lesson 2.

Fission barriers were calculated with the HF method using the Skyrme force [VB72] for the first time in 1973 [FQ73b, 74]. The obtained barrier heights do not agree with the experimental ones as well as those calculated with the shell-correction method; the reasons for this are mostly understood.

Nevertheless, it was a very essential step to prove that the double-humped barrier can be obtained in a purely microscopical approach.

2. HARTREE-FOCK (HF) THEORY OF NUCLEAR BINDING ENERGY

2.1 Effective nucleon-nucleon interaction: $V_{eff}(\underset{\sim}{r}_1,\underset{\sim}{r}_2)$

With $V_{eff}(\underset{\sim}{r}_1,\underset{\sim}{r}_2)$ we mean the interaction (potential,"force") which acts between two nucleons (placed at $\underset{\sim}{r}_1$ and $\underset{\sim}{r}_2$) in the nuclear medium, i.e. in the presence of the other nucleons of the same nucleus.

V_{eff} thus contains not only the basic interaction between the nucleons considered; it also summarizes the influence of the mutual interactions with all other nucleons of the same nucleus: Reduction of a many (A = N + Z)-body problem to a two-body problem.

Different from V_{eff} is the basic, so-called "free" nucleon-nucleon interaction $V(r_1,r_2)$ which acts between two isolated nucleons. With V one attempts to describe the scattering of two free nucleons by fitting phase shifts (phenomenological potentials V: e.g. Hamada and Johnston [HJ62]and Reid [Re68]. Theoretically, V can be derived from meson exchange processes (see e.g. [BJ76]).

The way from the free potential $V(r_1,r_2)$ to the effective one, $V_{eff}(r_1,r_2)$, in a finite nucleus is long and difficult: One has to solve a many (A)-body problem, which can only be done approximately. A succesful theory was developed by Brückner [Br55, Da67] for infinite nuclear matter; in the so-called "local density approximation" (LDA) [BG58, Be71] it could be applied to finite nuclei.

Extensive numerical calculations, starting with the "Reid soft core potential" $V(r_1,r_2)$ [Re68], were done in order to derive effective potentials $V_{eff}(r_1,r_2)$ which describe nuclear ground state properties well in the Hartree-Fock (HF) approximation (see below) [Ne70, CS72].

Another possibility is to design phenomenological effective interactions V_{eff} which have a simple mathematical form and adjustable parameters [Sk56, 59; Wi58, BB68, Mo70, KC73, NV70, EM72, Go75]. The most successful Hartree-Fock calculations were done in the last decade with the so-called Skyrme forces [Sk56,59], re-discovered by Vautherin and Brink[Va69, VB72, Va73] and further developed by the Orsay group [FQ73a,b; BF74, F175, Qu75a]. For extensive reviews of the results, see [F175,76; Qu75a,b]. A lecture series on the Skyrme forces was given in Trieste by Vautherin[1].

More recently, Gogny [Go73,75] developed a phenomenological force which allows also the self-consistent inclusion of pairing effects (Hartree-Fock-Bogolyubov method). This is probably at present the most refined effective force, which reproduces many nuclear groundstate properties extremely well.

The connection between the phenomenological Skyrme-type forces and the ones derived from the more basic Brückner-LDA-HF-calculations [Ne70, CS72] was made by Negele and Vautherin [NV72,75] : they justify not only the form, but also the approximate values of the parameters of the Skyrme force (see also [Ne75]).

[1] D. Vautherin, Trieste lectures 1975 (IAEA Vienna, 1975, SMR-14/39)

In the following, we summarize the HF theory; to study it, see e.g. the text book of G.E. Brown[1].

2.2 Hartree-Fock Approximation (HF)

We start from an effective two-body potential $V_{eff}(r_1,r_2)$. In general, it depends not only on the distance r_1-r_2 between the nucleons, but also on their velocities and on the local density $\rho(\frac{r_1+r_2}{2})$ of the nucleus.

The HF approximation consists in extracting from V_{eff} an average one-body potential $V_{HF}(r)$ in which the nucleons move independently. The wave-function[†] is written as an antisymmetrized product of single-particle wave-functions $\phi_i(\underset{\sim}{r})$:

$$\Phi_{HF} = \frac{1}{\sqrt{N!}} \det \left| \phi_i(\underset{\sim}{r}_j) \right|_{i,j=1,\dots N} \qquad \text{(Slater determinant)}. \tag{2.1}$$

The Hamilton operator is

$$\mathcal{H} = T + V_{eff} = \sum_{i=1}^{N} \frac{\hat{p}_i^2}{2m} + \sum_{i<j}^{N} V_{eff}(\underset{\sim}{r}_i, \underset{\sim}{r}_j, \hat{\underset{\sim}{p}}_i, \hat{\underset{\sim}{p}}_j). \tag{2.2}$$

The HF energy is then

$$E_{HF} = \langle \Phi_{HF} | \mathcal{H} | \Phi_{HF} \rangle . \tag{2.3}$$

2.3 Density matrix ρ

$$\rho_{\alpha\beta} = \sum_{i=1}^{N} \langle \alpha | i \rangle \langle i | \beta \rangle ; \qquad (2.4)$$

$|\alpha\rangle, |\beta\rangle$ is an arbitrary basis; $\langle\alpha|i\rangle$ are the expansion coefficients of the wavefunction $\phi_i(\underline{r})$ in this basis:

$$\phi_i(\underline{r}) = \sum_{\alpha} \langle \alpha | i \rangle \langle \underline{r} | \alpha \rangle . \qquad (2.5)$$

In terms of $\rho_{\alpha\beta}$, the HF energy (2.3) can be written as

$$E_{HF} = \sum_{\alpha\beta} T_{\alpha\beta} \rho_{\beta\alpha} + \frac{1}{2} \sum_{\alpha\beta} \sum_{\gamma\delta} \bar{v}_{\alpha\beta,\gamma\delta} \rho_{\delta\beta} \rho_{\gamma\alpha} , \qquad (2.6)$$

or, using matrix notation (tr ≡ trace)

$$E_{HF} = \mathrm{tr}\, T\rho + \tfrac{1}{2} \mathrm{tr}\left(\mathrm{tr}\, \bar{v}\rho\right)\rho . \qquad (2.7)$$

The matrices $T_{\alpha\beta}$ and $\bar{v}_{\alpha\beta,\gamma\delta}$ are the basic matrix elements:

$$\left.\begin{aligned} T_{\alpha\beta} &= \langle \alpha | -\tfrac{\hbar^2}{2m} \Delta | \beta \rangle \\ \bar{v}_{\alpha\beta,\gamma\delta} &= \langle \alpha\beta | v_{eff} | \gamma\delta \rangle - \langle \alpha\beta | v_{eff} | \delta\gamma \rangle . \end{aligned}\right\} \qquad (2.8)$$

[1] G.E. Brown, "Unified Theory of Nuclear Models", North Holland 1967

† We neglect spin and isospin coordinates and consider N nucleons of one kind only (e.g. neutrons).

The "best" set of s.p. wavefunctions $\phi_i(\underline{r})$ is found using the Ritz variational principle by minimizing the total energy E_{HF} with respect to the individual variations of all the ϕ_i:

$$\frac{\delta}{\delta \phi_i(\underline{r})} \left\{ E_{HF} - \varepsilon_i \int d^3\underline{r}\, |\phi_i(\underline{r})|^2 \right\} = 0 . \qquad (2.9)$$

The second term in the brackets { } is a Lagrange multiplier which guarantees the normalization of the $\phi_i(\underline{r})$. Performing the variation (2.9) leads to a set of equations:

$$\hat{H}_{HF} \phi_i = \left(\hat{T} + V_{HF}\right)\phi_i = \varepsilon_i \phi_i . \qquad \text{"HF equations"} \qquad (2.10)$$

In coordinate space, V_{HF} is in general a nonlocal, velocity-dependent potential, and the HF eqs. are very difficult to solve. (They are integro-differential equations).

In matrix notation, eq.(2.10) means a diagonalization :

$$H_{ij} = \varepsilon_i \delta_{ij} \qquad (i,j = 1, \ldots N) , \qquad (2.11)$$

and the matrix H is defined from (2.7) as

$$H_{\alpha\beta} = \frac{\partial E_{HF}}{\partial \rho_{\beta\alpha}} . \qquad (2.12)$$

If v_{eff} does not depend on the density, then V_{HF} in eq.(2.10) is equal to $\mathrm{tr}\,\bar{v}\rho$. T in eq.(2.10) is the kinetic energy operator $-\hbar^2/2m\,\Delta$.

For the Skyrme force, the HF equations are relatively simple†, of the type of a Schrödinger equation with an effective mass $m^*(\underline{r})$ and a spin orbit potential $\underset{\sim}{W}_{so}(\underline{r})$:

$$\hat{H}_{Sky}\phi_i(\underline{r}) = \left\{ -\underset{\sim}{\nabla} \cdot \frac{\hbar^2}{2m^*(\underline{r})} \underset{\sim}{\nabla} + U_{HF}(\underline{r}) - i \underset{\sim}{W}_{so}(\underline{r}) \cdot (\underset{\sim}{\nabla} \times \underline{\sigma}) \right\} \phi_i(\underline{r}) = \varepsilon_i \phi_i(\underline{r}) . \qquad (2.13)$$

The potentials U_{HF} and W_{so} and the eff. mass m^* depend in a relatively simple way on the local density $\rho(\underline{r})$ and the kinetic energy density $\tau(\underline{r})$ and thus the wavefunctions ϕ_i:

$$\rho(\underline{r}) = \sum_{i=1}^{N} |\phi_i(\underline{r})|^2 \; ; \quad \tau(\underline{r}) = \sum_{i=1}^{N} |\underset{\sim}{\nabla}\phi_i(\underline{r})|^2 . \qquad (2.14)$$

Through this dependence, the HF eqs. are non-linear and present a self-consistency problem. It is solved by starting from an initial set $\{m^{*(o)}, U_{HF}^{(o)}, W_{so}^{(o)}\} = H^{(o)}$; solving then eq.(2.13), from the ϕ_i calculating (2.14), from them new $H^{(1)}$ etc.etc.... until convergence, i.e. $H^{(n)} \equiv H^{(n+1)}$ (input ≡ output). ("HF iterations").

The ground state energy E_{HF} and wavefunction Φ_{HF} are obtained by including the N states ϕ_i with the lowest eigenvalues ε_i in the summations of eqs. (2.4) and (2.14).

2.4 Deformation energies

To obtain a solution with a given deformation, one has to add in eq.(2.10) an external field (constraint); otherwise one finds automatically a solution for which the energy is locally a minimum (ground state or eventually, an isomeric state).

The shape of the nucleus may be characterized by the multipole moments of the density:

$$Q_{\lambda\mu} = \mathrm{tr}\, \rho q_{\lambda\mu} ; \qquad (2.15)$$

here $q_{\lambda\mu}$ is the matrix element $\langle\alpha|\hat{q}_{\lambda\mu}|\beta\rangle$ of the multipole operator $\hat{q}_{\lambda\mu}$

$$\hat{q}_{\lambda\mu} = r^{\lambda} Y_{\lambda\mu}(\vartheta,\varphi) . \qquad (2.16)$$

Let us choose for instance the quadrupole moment $Q_{20} = Q_2$. If the HF equation

$$\left[\hat{T} + V_{HF} - \lambda \hat{q}_2\right]\phi_i = \varepsilon_i \phi_i \qquad (2.17)$$

† see the classical paper [VB72].

is solved, one obtains a solution with a quadrupole moment Q_2. The Lagrange multiplier λ gives then the local derivative of the deformation energy at the point Q_2 (i.e. the negative driving force, which wants to bring the nucleus back to the minimum):

$$\lambda = \frac{dE(Q_2)}{dQ_2} . \qquad (2.18)$$

In this way, one can, however, only obtain those regions of the curve $E_{HF}(Q_2)$ which have a positive curvature. To obtain the full curves, one can use a quadratic constraint (for details, see [FQ73a]) .

2.5. Main results of Skyrme-HF calculations : [F175,76; Qu75a,b]

Note: The Skyrme force has 6 adjustable parameters; for the pairing effects (in BCS approximation [Va73]) one more parameter is used. Thus, a total of 7 free parameters are used in all calculations.

1. Ground-state masses (binding energies) are reproduced within $\sim$2-5 MeV for spherical and $\sim$5-10 MeV for deformed nuclei. Nuclear radii (r.m.s.) fit within $\sim$2%; quadrupole moments of lanthanides and actinides within $\sim$2-4%.

2. Deformation energy curves: Have the correct qualitative properties. For Pu^{240}, a double-humped barrier was obtained, see Fig. 2.1 [FQ73b,74]. The barrier heights are too big, compared to the experimental ones. The differences are (mostly) due to the following shortcomings of constrained-HF-calculations:

- The HF equations are solved by diagonalization (eq.2.11) in a finite (truncated) harmonic-oscillator basis [Va73]. This leads to truncation errors in the total energy which affect the deformation dependence.

- Slater determinants (eq.2.1) are not good eigenstates of the centre of mass momentum and of the total angular momentum. This leads to spurious c.m. and rotational energies, which also affect the deformation-behaviour.

- For reasons of computer time, one must restrict the shapes to axial and left/right symmetry, which is known from Strutinsky-calculations to give too high barriers (see lesson 5).

- For the Coulomb exchange energy, the Slater approximation was used [NV72, Va73]; it was newly found to lead to an error which increases at larger deformations[1].

All the above deficiencies of the constrained HF method are (ideally) avoided in the Strutinsky method; see the following lessons.

Nevertheless, the merit of these HF calculations was to demonstrate that fission barriers can in principle be obtained purely microscopically. The HF calculations could furthermore be used to test and justify numerically the Strutinsky method [BQ73, 75a-d], see lesson 3.

[1] P. Quentin, private communication, 1978.

3. THE BASIS OF THE STRUTINSKY METHOD

3.1. Extraction of an average part of the HF energy :

We want to extract a smooth part of the HF energy, which varies slowly with particle number and deformation, as does the LDM energy. This means we want to derive microscopically the LDM from HF theory with effective interactions.

We saw in lesson 2 that the HF energy is given as a functional of the density matrix ρ (2.4), see expression (2.7) for E_{HF}. The proposition of Strutinsky [St68,74,75] was to split ρ into a smooth part $\tilde{\rho}$ which contains the average information (in the LDM sense) and an oscillating part $\delta\rho$:

$$\rho = \tilde{\rho} + \delta\rho : \qquad (3.1)$$

Without specifying $\tilde{\rho}$ quantitatively, Strutinsky derived [St68] what has been called the "energy theorem" [Be71](see also [BD72, BK72a, BK72b]), which we will discuss below. We give here a slightly different derivation (see also [Di72]); a discussion of different derivations may be found in [Br74b, BQ75a].

To define $\tilde{\rho}$ quantitatively, we use here Strutinsky's energy averaging method, which was originally introduced in order to define the average part of the single-particle level density of a given potential [St66-68]; see details in lesson 4. The same technique may be used to extract average parts of expectation values of any single-particle operator [BD72, BQ73], using the average occupation numbers $\tilde{n}_i$ determined by a given s.p. spectrum ε_i. The precise definition will be given in eq.(4.13) in the next lesson.

The average density matrix $\tilde{\rho}$ is defined as

$$\tilde{\rho}_{\alpha\beta} = \sum_i \langle\alpha|i\rangle\langle i|\beta\rangle \tilde{n}_i , \qquad (3.2)$$

thus replacing the "HF" occupation numbers (1 below and 0 above the Fermi energy λ) in eq.(2.4) by the $\tilde{n}_i$. This means an energy smoothing around the Fermi level λ in a range $\pm \sim\hbar\Omega$, the distance of main shell spacing in the spectrum ε_i.

The average part of any observable O - we are always speaking within the independent particle, i.e. HF approximation - is given through $\tilde{\rho}$ (3.2) and the corresponding operator $\hat{O}^{(1)}$ (one-body) or $\hat{O}^{(2)}$ (two-body) in matrix form:

$$\tilde{O} = \mathrm{tr}\,\tilde{\rho}\hat{O}^{(1)} \quad ; \quad \tilde{O} = \mathrm{tr}\left(\mathrm{tr}\,\tilde{\rho}\hat{O}^{(2)}\right)\tilde{\rho} . \qquad (3.3)$$

In terms of the HF matrix elements (e.g. one-body)

$$O_i = \langle i|\hat{O}^{(1)}|i\rangle$$

we thus get

$$\tilde{O} = \sum_i O_i \tilde{n}_i . \qquad (3.4)$$

The average density matrix in coordinate space $\tilde{\rho}(r,r')$ - the diagonal part of which is the ordinary density $\tilde{\rho}(r)$ - is

$$\tilde{\rho}(\underline{r},\underline{r}') = \sum_{\alpha\beta} \tilde{\rho}_{\alpha\beta} \langle \underline{r}|\beta\rangle\langle\alpha|\underline{r}'\rangle = \sum_i \phi_i(\underline{r})\,\phi_i^*(\underline{r}')\,\tilde{n}_i \,. \tag{3.5}$$

The average level density (see eq.(4.3)) is

$$\tilde{g}(E) = \frac{d}{d\lambda} \int d^3r\, \tilde{\rho}(\underline{r},\underline{r}) \Big|_E \,. \tag{3.6}$$

The average part of the HF energy E_{HF} (2.7) is thus simply

$$\tilde{\tilde{E}}_{HF} = \mathrm{tr}\, T\tilde{\rho} + \tfrac{1}{2}\,\mathrm{tr}\left(\mathrm{tr}\, \bar{v}\tilde{\rho}\right)\tilde{\rho} \,. \tag{3.7}$$

(If the interaction V depends itself on ρ, it is understood in eq.(3.7) that it has to be taken at the average value $\tilde{\rho}$!)

By construction, $\tilde{E}_{HF}$ should behave like a LDM energy. Numerical checks see below.

3.2. The Strutinsky Energy Theorem

(see also [St68,74,75; BD72, BK72a,b; Di72, Be71, Br74b, BQ75a]).

The aim is to derive from the microscopical HF-theory a quantitative expression for the fluctuating part δE of the total nuclear binding energy, see eq.(1.2), that is, for the shell-correction.

The easiest way is to expand the HF energy functional $E_{HF}[\rho]$ eq.(2.7) around the average part of ρ:

$$E_{HF}[\rho] = E_{HF}[\tilde{\rho}] + \mathrm{tr}\left(\frac{\partial E_{HF}}{\partial \rho}\Big|_{\rho=\tilde{\rho}} \delta\rho \right) + \mathcal{O}[(\delta\rho)^2] \,. \tag{3.8}$$

This Taylor expansion is - hopefully ! - justified by the relative orders of magnitude of the average (LDM) energy ($\sim$ 1-2 GeV) and the shell-correction ($\pm \sim$5-15 MeV).

The first term on the r.h.s. of eq.(3.8) is identical to $\tilde{\tilde{E}}_{HF}$ (3.7). The second term contains the derivative of E_{HF} with respect to ρ - which is a matrix - and which is equal to the HF one-body Hamiltonian H_{HF} (2.12) taken at the smooth value of ρ . We call it

$$H_{HF}[\tilde{\rho}] = \tilde{H}_{HF} = \hat{T} + \tilde{V}_{HF} \,. \tag{3.9}$$

We have thus

$$E_{HF} = \tilde{\tilde{E}}_{HF} + \mathrm{tr}\, \tilde{H}_{HF}\delta\rho + \mathcal{O}[(\delta\rho)^2] \,. \tag{3.10}$$

Now, the difference between V_{HF} and $\tilde{V}_{HF}$ is of order $\delta\rho$ and thus small relative to V_{HF} :

$$\delta V_{HF} = V_{HF} - \tilde{V}_{HF} = \mathcal{O}[\delta\rho] \,. \tag{3.11}$$

Let us call the spectrum and eigenstates of $\tilde{V}_{HF}$: $\tilde{\varepsilon}_i$ and $\tilde{\phi}_i$ respectively:

$$\tilde{H}_{HF}\tilde{\phi}_i = \left[\hat{T} + \tilde{V}_{HF}\right]\tilde{\phi}_i = \tilde{\varepsilon}_i\,\tilde{\phi}_i \,. \tag{3.12}$$

Using perturbation theory, we find easily that

$$\mathrm{tr}\, \tilde{H}_{HF}\delta\rho = \sum_i \tilde{\varepsilon}_i\,\delta\tilde{n}_i + \mathcal{O}[(\delta\rho)^2] \,. \tag{3.13}$$

[The $\delta\tilde{n}_i$ are defined in terms of the average spectrum $\tilde{\varepsilon}_i$ and not identical to those obtained from the HF spectrum ε_i, unless the averaging is done self-consistently by iteration; see below. We ignore the difference, however, which is again of higher order.] The quantity in eq.(3.13) is thus just the usual shell-correction (see lesson 4, eq. 4.14) :

$$\delta E_1 = \sum_i \tilde{\varepsilon}_i\,\delta n_i = \sum_{i=1}^{N} \tilde{\varepsilon}_i - \sum_i \tilde{\varepsilon}_i\,\tilde{n}_i \,. \tag{3.14}$$

We arrive thus at the Strutinsky energy theorem

$$E_{HF} = \tilde{E}_{HF} + \delta E_1 + \delta E_2 + \ldots \tag{3.15}$$

The important point is that all shell effects of lowest (i.e. first) order in $\delta\rho$ are given by expression (3.14); the remaining higher-order terms should be small (δE_2 etc).

The practical importance of this is that δE_1 is given by the spectrum ($\tilde{\varepsilon}_i$) of an average potential $\tilde{V}_{HF}$ (3.12), which may be approximated by the standard (deformable) shell model potential V_{SM} (which by construction varies smoothly with N, Z and deformation!). With this assumption one does not need to know the effective interaction v_{eff} for calculating δE to lowest order. (The terms of $\delta E_2, \ldots$ depend explicitly on v_{eff}!). If, furthermore, E_{HF} is close to the LDM energy E_{LDM} and the higher order terms $\delta E_2, \ldots$ are negligible, the approximation (SCM = shell correction method)

$$E_{SCM} = E_{LDM} + \delta E_1 \tag{3.16}$$

should replace a HF calculation, which in the later sixties was not available for fission barriers!

[We left out here the pairing effects. In principle the energy theorem can be derived from HFB-theory, [see Ko73]].

The derivation of the energy theorem (3.15) given here is true for any density and velocity-dependent effective two-body interaction v_{eff}.

3.3. Basic assumptions of the Shell-Correction Method (SCM)

1. The average HF energy $\tilde{E}_{HF}$ can be parametrized and well approximated by the LDM energy E_{LDM} (in the form e.g. eq.(1.1)), both as a function of nucleon numbers N, Z and of deformation β. In particular, it should thus

be a smooth function of N, Z and β (no shell effects).

2. The average HF potential $\tilde{V}_{HF}$ can be well approximated by a phenomenological shell model potential V_{SM} (Nilsson, Woods-Saxon etc). What counts is not so much the radial dependence of $V_{SM}(r)$, but that the shell-correction δE_1 extracted from its spectrum is the same as that obtained from $\tilde{V}_{HF}$.

3. The higher-order shell-corrections $\delta E_2 \ldots$, are small compared to δE_1 (i.e. $|\delta E_2| < 1\text{-}2$ MeV), so that they can be neglected.

If these assumptions are true, the energy E_{SCM} (3.16) replaces the HF-energy.

3.4. Numerical test of the SCM with HF-calculations

(see [BQ73-75], also [BK73]).

Idea: Perform numerically the program used above to derive the energy theorem and check individually each term.

Results: Figs. 3.1 and 3.2 show deformation energy curves obtained with HF calculations (interactions Skyrme III [BF74] and Negele-DME [NV72]) with a constraint on the quadrupole moment Q_2. The average energy $\bar{E}(= \tilde{E}_{HF})$ is seen to behave exactly like a smooth LDM energy. Shown also is the LDM energy E_{LD} with the parameters of [MS66]. The differences between $\bar{E}$ and E_{LD} could easily be removed by a re-adjustment of the LDM parameters.

Fig. 3.3 shows shell-corrections δE_1 and δE_2; the latter is found as $\delta E_2 = E_{HF} - \tilde{E}_{HF}$ and contains thus all higher-order terms. δE_1 agrees for both interactions and also with the one found in a usual Woods-Saxon potential [BD72] (no adjustment of parameters!) within $\sim$1-1.5 MeV. $|\delta E_2| \lesssim 2$ MeV everywhere; the oscillations are only $\pm \sim$1-1.5 MeV.

Fig. 3.4 shows the sum of 2. and higher order shell-corrections, δE_2, for 14 different nuclei with $100 \lesssim A \lesssim 250$ in their groundstates. The average value of δE_2 is $\sim$2 MeV and could easily be renormalized into the LDM energy; the fluctuations in δE_2 are less than $\pm \sim$1 MeV.

More results, see [BQ73-75].

Conclusions:

1) The series $E_{HF} = \tilde{E}_{HF} + \delta E_1 + \delta E_2 + \ldots$ converges very rapidly. In nuclei with $A \gtrsim 100$, $|\delta E_2|$ is always less than $\sim$ 2 MeV; its oscillations are less than $\pm \sim$1-1.5 MeV.

2) The shell-correction δE_1 is well reproduced by a phenomenological shell-model potential within $\pm \sim$1-1.5 MeV; it seems to depend little on the effective interaction.

3) The average energy $\tilde{E}_{HF}$ ($\bar{E}$ in figs. 3.2, 3.3 and 3.6 below) has the features of a LDM energy: Minimum at spherical shape, no rapid oscillations (shell structure). It can be fitted by a standard LDM energy within less than $\sim$ 1 MeV.

4) In light nuclei, δE_2 is not small, but of the same order as δE_1 (see [BQ75a,c]). Thus: attention for shell-correction calculations with not-self-consistent potentials for light nuclei!

5) Since all these differences of $\sim$1-2 MeV seem to be rather random (not in phase as functions of N, Z and Q_2), they should normally not add up. Thus, in heavy nuclei, the total error (compared to a self-consistent HF calculation) should not exceed $\sim$1-2 MeV.

6) If the average quantities $\tilde{\rho}$, $\tilde{E}_{HF}$ and $\tilde{V}_{HF}$ are determined self-consistently (by iteration), then $|\delta E_2|$ is less than 0.5-1 MeV for all N, Z and Q_2 tested [BQ75b]. The approximation

$$E = \tilde{E}_{HF} + \delta E_1(\tilde{\epsilon}_i) \qquad \text{(self-consistent)} \quad (3.17)$$

converges thus extremely well. This is even the case for light nuclei, see e.g. ^{40}Ca in Fig. 3.5!

7) The ideal shell-correction method should thus use LDM parameters and shell-model potentials $\tilde{V}$ which are determined self-consistently from one and the same effective interaction V_{eff}. This needs to be done!

8) All these results are derived from the HF framework. For tests with Migdal's theory, which exceeds in principle the HF-approximation, see [BK72a].

9) Self-consistency is important mostly for the average energy and potential. The shell-effects can be treated perturbatively. This motivates the use of semiclassical methods to solve the average self-consistency problem with a given interaction (see e.g. [BC76, CJ77]).

4. PRACTICAL DETAILS OF THE SHELL-CORRECTION METHOD

The "program" of a Strutinsky calculation is summarized in the following.

1) Parametrization of nuclear shape $\{\beta_i\}$
2) Parametrization of LDM energy
3) Parametrization of shell-model potential
4) Calculation of the shell-correction δE; pairing correction δP
5) Add up: $E_{def}(\beta_i) = E_{LDM}(\beta_i) + \delta E(\beta_i) + \delta P(\beta_i)$ †)

We cannot possibly mention all the different choices of parameters and potentials, which were used by different groups. Table 4.1 shows a list of the most active groups (especially in the years 1968-1974) and their potentials.

We go quickly through the above points, mention only the essentials and refer to literature for details. Good review articles, covering both technical details and results are [TN70, BD72, Ni72, Pa73, MN73].

† We omit from now on the index "1" used in lesson 3 to denote the first order shell-correction δE_1

For illustrative examples, we shall use nomenclature and results of the Strutinsky group (Moscow-Copenhagen-Basel), published in [BD72].

4.1. Shape parametrization

From the LDM studies, we have learned that the two most important degrees of freedom in the fission process are:

1) Elongation of the nucleus (c)
2) Neck-formation (constriction) (h)

In accordance with LDM results, these deformations are always chosen axially symmetric (around the fission axis) and left-right (mass-)symmetric (with respect to a perpendicular plane through the neck).

In the Copenhagen-Basel [BD72] and Los Alamos [Ni72] groups, these two degrees of freedom were parametrized such as to closely reproduce the family of optimized saddle-point shapes obtained in the numerical LDM calculations [CS63, SL63]. In the {c,h} parametrization [BD72], the LD fission path goes (for actinides) approximately along $h \neq 0$. The {c,h} shapes are shown in Fig. 4.1 by the solid lines. (Spherical shape: $c = 1.0$, $h = 0$).

In Nilsson-model and related potentials, these two degrees are reproduced by a mixture of ε_2, ε_4 and ε_6 deformations. Close to sphericity, $c \sim \varepsilon_2$ and $h \sim \varepsilon_4$.

The other two important types of deformations, which do not occur in the statistical LDM and are pure shell effects, are:

3) left/right (mass-, octupole-) asymmetry (α)

4) non-axial (tri-axial ellipsoid), γ-deformation

The asymmetry (α) is defined quite differently from group to group (Lund: a mixture of ε_3 and ε_5). γ is always the traditional tri-axial deformation parameter.

4.2. LDM energy

At early stages, the classical parameters of Myers and Swiatecki [MS66] were used. Later (> 1969), all groups oriented themselves more or less towards the "droplet model" [My69, MS69] ; with details to be found in the different references.

The essentials of the LDM deformation energy have already been discussed in lesson 1.

4.3. Shell model potential (deformed) V(r)

We give here the potentials of the main groups, with references for details:

1) Nilsson-model: (modified harmonic oscillator) with $\varepsilon_2 - \varepsilon_6$ and γ deformations: [St66-68, NT69, Mö72, MN73]

2) Two-centre-model: (two joined harmonic oscillators): [GM71, SG71, SM72, AD72, MM73, Ju74].

3) "folded Yukawa potential" (a deformable density with sharp surface, folded with a short-range Yukawa force to generate a diffuse surface) : [Ni69, BF72, Ni72, MN73].

4) generalized Woods-Saxon potential with constant surface thickness: [DP69a,b; BD72, GP72, Pa73, BL74, Ju75, JH77].

Some main common points are:

- The surfaces of constant potential V(r) (but, due to lack of self-consistency, not necessarily exactly of constant density!) are chosen to be the same as those of the drops (droplets) of the corresponding LDM.

- The volume within an equipotential surface is independent of deformation (incompressibility of nucleus).

In fig. 4.2 we see an example of the single-particle levels ε_i for the deformed Woods-Saxon potential of ref. [BD72, Pa73].

4.4. The Strutinsky energy averaging method [St66-68; Ts69, BP73].

This is the main technical ingredient of all practical shell-correction calculations. There exists a wide literature of descriptions, criticisms and alternative suggestions. The situation up to spring 1975 is covered in [BQ75a]; we refer to this paper and to [Br74b] for most of that literature and present here only shortly the main points.

One wants to define the average part of the total single-particle energy E_{sp} of one kind of particle:

$$E_{sp} = \sum_{i=1}^{N} \varepsilon_i . \tag{4.1}$$

This is done over the level density

$$g(E) = \sum_i \delta(E-\varepsilon_i) . \tag{4.2}$$

The smooth level density $\tilde{g}(E)$ is defined by averaging the exact one over an energy range γ with a certain averaging function $f_M(\chi)$:

$$\tilde{g}(E) = \frac{1}{\gamma}\int_{-\infty}^{+\infty} dE' g(E') f_M\left(\frac{E-E'}{\gamma}\right) = \frac{1}{\gamma}\sum_i f_M\left(\frac{E-\varepsilon_i}{\gamma}\right). \tag{4.3}$$

(M is an even integer, see below).

The function $f_M(\chi)$ has the following properties [BP73]:

1) $f_M(\chi)$ is even in χ, has its maximum at $\chi = 0$ and goes to zero for $\chi \to \pm\infty$

2) Folding an arbitrary polynomial $P_M(E)$ (of degree M) leaves this polynomial unchanged for any value of γ :

$$\frac{1}{\gamma}\int_{-\infty}^{+\infty} P_M(E')\, f_M\left(\frac{E-E'}{\gamma}\right) dE' \equiv P_M(E). \qquad (\forall\,\gamma) \tag{4.4}$$

3) In the limits $\gamma \to 0$ and $M \to \infty$, $f_M(\chi)$ gives a delta function:

$$\frac{1}{\gamma} f_M(\chi/\gamma) \xrightarrow[\text{or } M\to\infty]{\gamma\to 0} \delta(\chi). \tag{4.5}$$

In order to smooth out the shell effects in (4.2), one has to choose γ slightly larger than the distance $\hbar\Omega$ of the main shells in the spectrum:

$$\gamma \gtrsim \hbar\Omega. \tag{4.6}$$

Fig. 4.3 shows as an example the level density g(E) for a deformed Woods-Saxon potential [BD72]. The dashed lines are the averaged level densities $\tilde{g}(E)$.

The condition (4.4) guarantees that the results do not depend on γ if the (true) average part of g(E) is a polynomial of degree M.

The average single-particle energy $\tilde{E}_{sp}$ is now given by

$$\tilde{E}_{sp} = \int_{-\infty}^{\tilde{\lambda}} E\,\tilde{g}(E)\, dE, \tag{4.7}$$

where the Fermi energy $\tilde{\lambda}$ is determined by

$$N = \int_{-\infty}^{\tilde{\lambda}} \tilde{g}(E)\, dE. \tag{4.8}$$

If the (true) average density $\tilde{g}(E)$ is a polynomial of degree M_0, then the energy $\tilde{E}_{sp}$ (4.7) will not depend on γ as soon as $M > M_0 + 2$ and eq.(4.6) is fulfilled. If the spectrum ε_i is unlimited, then the function $\tilde{E}_{sp}(\gamma)$ has an ideal "plateau" in the region

$$\hbar\Omega \lesssim \gamma \ll \tilde{\lambda} - \varepsilon_0. \tag{4.9}$$

This is the case for the harmonic oscillator potential (in 3 dimensions: $M_0 = 2$), see Fig. 4.4. It is also approximately true for Nilsson-model potentials: the plateau is constant within $\sim \pm 0.2$-0.3 MeV.

For an arbitrary average density, the Strutinsky procedure approximates the average part locally into a Taylor series which stops after M/2 + 1 terms. The error is minimised by the "local plateau condition" [BP73] for γ

$$\frac{\partial \tilde{E}_{sp}}{\partial \gamma} = 0 \tag{4.10}$$

and for M:

$$\tilde{E}_{sp}(M) = \tilde{E}_{sp}(M+2). \tag{4.11}$$

In Fig. 4.5 is an example where eqs.(4.10, 11) are only fulfilled for $M \gtrsim 16$; this is rather exceptional. In most cases, local plateaux are found with $6 < M < 10$ and $\hbar\Omega \lesssim \gamma \lesssim 1.5\ \hbar\Omega$.

In potentials with finite depth (e.g. Woods-Saxon), the range γ may reach into the continuum region (E > 0). There, ideally the resonances should be included [RB72]. In praxis, one uses artificial unbound states up to $\sim$ + 20 MeV which are obtained by diagonalizing the potential in a harmonic oscillator basis. In doing so, the uncertainties in the plateau values of E_{sp} are usually not larger than $\sim$1-1.5 MeV. In some exceptional cases, especially at larger deformations with high local level density[1,2] - see e.g. Fig. 4.6 at c = 1.6 and 1.72 - or for small nuclei where $\hbar\Omega$ is bigger than the distance of λ from the continuum [SG77] ($A \lesssim 80$-100), the uncertainty may be somewhat larger.

At the plateau point where eq.(4.10) is fulfilled, the smooth energy $\tilde{E}_{sp}$ (4.7) can also be written as

$$\tilde{E}_{sp} = \sum_i \varepsilon_i \tilde{n}_i \tag{4.12}$$

with the smooth occupation numbers $\tilde{n}_i$ being defined by

$$\tilde{n}_i = \int_{-\infty}^{(\tilde{\lambda}-\varepsilon_i)/\gamma} dx\, f_M(x). \tag{4.13}$$

[1] R.R. Chasman, Phys. Rev. Lett. 33 (1974) 544
[2] V.S. Ramamurthy et al. Phys. Lett. 62B (1976) 124

The shell-correction is thus

$$\delta E = E_{sp} - \tilde{E}_{sp} = \sum_i \varepsilon_i \delta n_i, \tag{4.14}$$

where

$$\delta n_i = n_i^{(0)} - \tilde{n}_i\ ; \qquad n_i^{(0)} = \left\{ \begin{array}{ll} 1 & \\ 0 & \text{for } i > N \end{array} \right\} \quad i = 1,2,\ldots N. \tag{4.15}$$

In Fig. 4.7 we show the values of δn_i in a typical case (the value of δn_i is the length of each vertical line, located at the energy ε_i). That figure also demonstrates that the shell-correction δE is mostly determined by the levels inside an interval $\tilde{\lambda} \pm \sim\gamma$. Thus, the deep-lying levels do not contribute to δE (4.14).

Of various methods proposed as alternatives to the Strutinsky averaging (see references in [BQ75a]), the only one which completely avoids the continuum problem is the semiclassical method developed by Bhaduri and Jennings [BR71, Je76]. Detailed comparisons of both methods show that they lead to identical results within $\sim$1-2 MeV [JB75b,c], thus essentially confirming the Strutinsky method using artificial unbound states in finite potentials.

Strutinsky and Ivanjuk [SI75] proposed a modified averaging method which uses only bound states. Here, too, some uncertainties in the plateau values of $\tilde{E}_{sp}$ of $\sim$1-1.5 MeV are found. Improvements of this method seem, however, possible [SB77][1].

4.5. Pairing correlations

They have to be included in medium and heavy nuclei. This is done in the BCS formalism; a pairing correction is calculated (δP) which is determined as the ocsillating part of the difference between a paired and an unpaired ($\Delta = 0$) system. Definitions see [BP72, Pa73].

4.6. Numerical uncertainties in the shell-corrections (in praxis)

a) due to numerical energy averaging: (this lesson)

- in infinite potentials (Nilsson, square box) : $|\Delta\tilde{E}| < 0.5$ MeV
- in finite potentials (Woods-Saxon, folded Yukawa):

  for $A \gtrsim 100$: $|\Delta\tilde{E}|$ usually $\lesssim$ 1-1.5 MeV
  for light nuclei, or in situations with extremely high level density (e.g. at second barrier without mass-asymmetry):
  $|\Delta\tilde{E}|$ maybe $\sim$ 1.5-2.5 MeV (?)

b) due to lack of self-consistency of potential used :

(see lesson 3)

- in heavy nuclei and deformations up to second fission barrier:

[1]see also Ivanjuk and Strutinsky, Kiev-preprint (1978)

$|\Delta\delta E| \lesssim$ 1-1.5 MeV

- in light nuclei: up to several MeV!
- at very large mass asymmetry and large separation (mostly in application to heavy-ion-reactions) :[1,2]

  $|\Delta\delta E|$ up to several MeV!

c) due to lack of self-consistency between potential and LDM:

- $|\Delta\delta E|$ easily $\sim$2-3 MeV; but smooth as function of N, Z and deformation!
- "Pb-anomaly" : $\Delta\delta E \sim -4$ to -7 MeV !! (see lesson 5)

This error can be removed by a renormalization of the LDM parameters. It does not occur, if the potential V(r) and the LDM parameters are derived from the same effective interaction and self-consistently [BQ75b] (see also lesson 3) - but this has not been done in the praxis so far!

[1] P. Möller and J.R. Nix, Nucl. Phys. A281 (1977) 354
[2] H. Gick et al., Z. Physik A282 (1977) 417

5. RESULTS OF SCM CALCULATIONS

In this lecture we will summarize the results of realistic deformation energy calculations using the SCM. As illustrations, we will show some typical results which we have taken - for pure convenience - from refs. [BD72, Pa73]. Unless particularly stated otherwise, all the results discussed here have been obtained independently and with excellent overall agreement by the different groups using different potentials, as discussed in sect. 4.3.

We shall restrict ourselves to static aspects, since the dynamics of fission is still at a rather early theoretical stage. The only exception will be the fission life time estimates (sect. 5.6), where a "minimal dynamical information" is needed in the form of inertial parameters; there, too, the static deformation energy is however the main ingredient.

5.1. Deformation energy surfaces

The basic problem in representing the deformation energy of a nucleus is that the deformation space $\{\beta\}$ has an infinite dimensionality. One thus has to select the most important deformation degrees of freedom - mostly using intuition.

From the LDM calculations (see sect. 1.2) we know that elongation (c) and necking (h) are important collective modes during the fission process. A practical way towards an approximate solution of the multidimensional problem consists in calculating the deformation energy E(c,h) and minimizing it at each point (c,h) with respect to other possible deformations.

Fig. 5.1 shows as examples the energy surfaces E(c,h) obtained in ref. [BD72] for the nucleus Pu^{240} for axially and mass symmetric shapes ($\gamma = \alpha = 0$). The contributions E_{LDM}, δE_n and δE_p (including pairing) are shown separately; on the lower r.h.s. is the sum of the three, i.e. the total energy (normalized, as usual, to $E_{LDM}(0) = 0$). Note that the inclusion of the shell effects moves the ground state minimum to a deformed shape ($c \simeq 1.2$, $h \simeq -0.15$). At the same time, a secondary minimum is created ($c \simeq 1.4$, $h \simeq 0$) which lies about 2 MeV above the ground state and is separated between ground state and the fission valley by two saddles.

This secondary minimum is found in most actinides and explains the nature of the long-known fission isomers [Po62] as shape isomers. Their deformation corresponds roughly to that of an ellipsoid with axis ratio 2/1. The shapes of the four stationary points in this symmetric energy surface E(c,h) are shown in Fig. 5.2.

Spontaneous fission from the second minimum is much more likely (only one barrier) than from the ground state (two barriers, lower energy). Thus, the fission life times from isomers are typically 10^{20}-10^{22} times shorter than those from ground states.

We shall return later to some of the consequences of the existence of these fission isomers (sect. 5.4).

5.2. Influence of non-axial and mass-asymmetric deformations

When mass-asymmetric shapes ($\alpha \neq 0$, see Fig. 4.1) are included, one finds that in the region around the second saddle point and beyond it, the energy is lowered by several MeV. The energetically most favorable path leads thus over a mass-asymmetric second saddle. This is a pure shell effect (in the LDM α is always zero!) and indicates the building up of asymmetric fragments.

Fig. 5.3 shows the second saddle region; in the upper part with $\alpha = 0$ and in the lower part after minimizing E with respect to α in each point (c,h). Note that the barrier height is decreased by $\sim$2.5 MeV! The isomer minimum is stable ($\alpha = 0$). The mass asymmetry thus increases rapidly between the isomer minimum and the outer saddle; beyond the saddle it stays constant in such a way that the ratio of the nascent fragments approaches a more or less constant value as the nucleus approaches the scission point. This value agrees qualitatively well with the most probable mass ratio observed in the fragment distribution. (For a recent comparison, see [JH77]).

This is particularly well demonstrated in a calculation using the two-centre-model (see sect. 4.3) which is especially well suited for the shapes between saddle and scission point. Fig. 5.4 shows as an example the energy surface of U^{236} as a function of neck radius (D) and mass asymmetry [MM73]. One sees the valley which leads down from the saddle with an approximately constant mass ratio ($\sim$140:96 near scission). The fact that this agrees well with the experimental (most probable, kinetic energy averaged) mass ratio, should of course be taken with caution. Here we considered only the potential energy (i.e. static) aspect of the problem, ignoring dynamical (inertial) effects which may play an important role especially on the way down towards scission!

Still, it is interesting that the mass ratio of the future fragments is already indicated after the saddle point by a purely static shell effect.

Another important deformation degree of freedom is the non-axial (γ) deformation. In the same way as mass asymmetry lowers the second saddle, one finds that inclusion of γ-deformation lowers the first saddle by up to $\sim$2 MeV for actinides with $A \gtrsim 232$. This effect, which increases through the actinide region with increasing mass number, considerably improves the agreement between theoretical and experimental heights of the first barrier (see e.g. Fig. 11 in ref. [MN73](Rochester) p.125).

Recently, an instability against γ-deformation was also found around the second barrier [GB77, JH77]. It leads to a "second outer" saddle which is γ-deformed but mass symmetric and lies $\sim$1-2 MeV higher than the usual, mass asymmetric but axially symmetric outer saddle. This "new channel" may affect the fission cross section at larger excitation energies (see [GB77]), especially in the mass-symmetric mode.

5.3 Systematics of barrier heights

We refer to the lectures of E. Lynn[1] for the extraction of barrier heights from an analysis of fission cross sections. In Fig. 5.5 we see a comparison[1] of the most up-to-date experimental barrier heights (E_A = inner, E_B = lowest outer barrier) with the theoretical values obtained using three different shell model potentials (see sect. 4.3).

In general, there is a pretty good agreement, amongst the different theoretical results as well as between theory and experiment. A systematic deviation is found for E_A in light actinides with low neutron number ($N \lesssim 140$). This discrepancy, first observed in Th-isotopes, has obtained the name "Th-anomaly". Otherwise, the calculated barriers agree with the experimental ones within $\sim$1-2 MeV. As we have seen in the previous lesson (sect. 4.6), this is the general kind of uncertainty which we expect in SCM calculations; so we cannot expect the agreement to be much better.

A possible explanation of the Th-anomaly may be the fact that in some calculations [MN73] a splitting of the second barrier into two small humps, separated by a shallow (third) minimum, has been found. This would completely change the analysis of fission cross sections (see Lynn's lectures). However, the fluctuations of this split second barrier are only of the order of $\sim$1-2 MeV, and have thus to be taken with caution. Furthermore, it seems that the picture of the triple-humped barrier (with a second minimum at $\sim$2-3 MeV and a third minimum at $\sim$4-5 MeV) is not compatible with photofission data of Th^{232} [2,3]. (See lesson 6 for more discussion about Th).

5.4 Physics of the fission isomers

We quickly summarize here the kind of experiments that allow to learn about the nature and details of the fission isomers. Extensive reviews were given by Specht [Sp74][4].

a) The fission cross sections (excitation functions) are modified by the isomers in a characteristic way: they show resonances which correspond to vibrational states in the second well. (See the lectures of Lynn for details).

b) The rotational band built on the lowest 0^+ state in the second well of Pu^{240} was measured in a rather spectacular experiment [SW72]. The deduced moment of inertia $\mathcal{J}$ is about 2.5 times larger than that of the g.s. band. This was the first direct evidence of the large deformation of an isomer. The measured value of $\mathcal{J}$ agrees well with the theoretical one, obtained from the single particle wavefunctions with the cranking model (although the latter one has an uncertainty of $\sim$5-10%). A similar experiment was recently finished for U^{236} [BP77a].

c) The most direct determination of the deformation of an isomer was obtained in a recent measurement of the quadrupole moments Q_2 of Pu^{239} [HM77] and Pu^{236} [MS77] in the isomer state. The agreement of Q_2 (within the experimental error limits) with the theoretical values [BL74] is excellent.

[1] E. Lynn, these proceedings

[1] D. Habs et al., Heidelberg Preprint 1978 (Z. Physik, in press).
[2] C.D. Bowman et al., Phys.Rev. C17 (1978) 1086.
[3] M. Asghar, Z. Physik A, in print (1978).
[4] and H. Specht, Nukleonika Vol. 20 (1975) 717 (Summer School Mikolajki, 1974).

d) The only directly (and precisely) measured energy of the fission isomeric state known up to date is the one of U^{238}, deduced from observed γ-transitions between the 0^+ state in the second well and the lowest 2^+ and 1^- states in the ground state well[1]. The energy $E_{II}-E_I$ = 2.559 MeV agrees well with the theoretical values within their error limits.

e) Spectroscopy in the isomeric well was attempted for Pu^{237} [2]. Here, two isomeric states are known with half lives 100 ns and 1.1 μs. Since this is an odd-A nucleus, these states have spin J, K ≠ 0. Their g-factors were measured with the spin-precession method in an external field. The spin assignments were, however, not unique.

5.5. Ground-state masses

The SCM can of course also be used to calculate the total ground-state mass (binding energy) of a nucleus. The empirical corrections δM to the LDM energies were determined systematically for the first time by Myers and Swiatecki [MS66]. More recent compilations, using different versions of semi-empirical mass formulae or the droplet model[3], may be found in Nuclear Data Tables[4]. In Fig. 5.6 we see a comparison of the empirical values of δM^3 with the theoretical ones, obtained with the folded Yukawa potential [MN73]. The agreement is in general good, within ± ∿1-2 MeV, except in the Pb region. Especially using a Woods-Saxon potential [BD72], one obtains a discrepancy of ∿5 MeV for Pb^{208}.

This "Pb-anomaly" is much smaller, when one uses the Nilsson model. In the most recent mass fit using Nilsson levels[5], an agreement
$-2\ \text{MeV} \lesssim (\delta M_{th} - \delta M_{exp}) \lesssim +2\ \text{MeV}$ was reached (although here, too, the most systematic deviations occur around Pb^{208}). On the other hand, the too large (negative) value of δM obtained for Pb^{208} with the Woods-Saxon potential has been substantiated[6] by HF-calculations [BQ75b] in which the exact total energy of Pb^{208} is reproduced. The discrepancy must therefore be due to the lack of self-consistency between the smooth (LDM) energy and the W-S. potential used. This is the point we made at the end of sect. 4.3 above (point c).

If both the average energy and the average potential are derived self-consistently from the same interaction, as was done in ref.[BQ75b], the Pb-anomaly does not exist; see the results discussed in sect. 3.4, especially point 6), and eq.(3.17)! It is possible that the Th-anomaly discussed above is due to the same reason.

[1] P.A. Russo et al., Rochester 1973, Vol. I, p.271.
[2] R. Kalish et al., Phys. Rev. Lett. 32 (1974) 1009.
[3] W.D. Myers and W.J. Swiatecki, Ann. Phys. (N.Y.) 84 (1974) 186.
[4] Atomic Data and Nuclear Data Tables, Vol. 17 (1975) 411.
[5] P.A. Seeger and W.M. Howard, Nucl. Phys. A238 (1975) 491
[6] see also Y. Yariv et al., Z. Physik A278 (1976) 225.

5.6. Life time estimates for spontaneous fission

We just sketch here a simple semiclassical method which allows to calculate life times using WKB barrier penetration. The first systematic studies of this kind were done by Ledergerber and Pauli[1] [PL73]. For more recent similar studies, see refs.[2,3]

If the fission path is represented as a one-dimensional trajectory q(c,h,a...) in the deformation space, the probability (width) Γ for barrier penetration between points q_1 and q_2 is in the WKB approximation (see e.g. [BW39])

$$\Gamma \simeq \hbar\omega_f \cdot e^{-\frac{2}{\hbar}S} \qquad (S \gg \hbar),$$

where $\hbar\omega_f \approx 1$ MeV (within a factor of ∿2) is the frequency of "assault" in the fission mode (q), and S is the action integral along the chosen trajectory:

$$S = \int_{q_1}^{q_2} \sqrt{|E-V(q)|\,2B_q(q)}\; dq .$$

Here V(q) is the potential energy of collective deformation, i.e. the deformation energy obtained with the SCM along the path q(c,h,α...); $B_q(q)$ is the inertial parameter which in the adiabatic approximation can be obtained using the "cranking model" [4]; E is the total energy of the system.

The most probable path is the one which minimizes the action S, i.e. the "least action trajectory". An example of such a trajectory is shown in Fig. 5.7 (from [PL73]).

This method applies only if one is well below the barrier; it can therefore only be used with reasonable justification for spontaneous (g.s. or isomeric) fission. Hereby, q_1 is a point in the g.s. (or isomeric) minimum and q_2 a point in the "fission valley" on the other side of the barrier at the same energy. The life time is then given simply by

$$t_{1/2} \simeq \frac{\hbar}{\Gamma} .$$

Since Γ is extremely sensitive to the barrier heights (through the exponential dependence), the inaccuracy in the latter (∿1-2 MeV) leads to theoretical error limits in $t_{1/2}$ of several orders of magnitude.

Fig. 5.8 shows the results obtained in [PL73] for ground state fission of the actinides. (Hereby, the LDM parameters a_s and κ_s were readjusted in three different regions, as shown in the figure). There is a very clear correlation between theoretical and experimental values within each isotope series.

Similar results were obtained by Randrup et al.[2] using a phenomenological (classical) inertial function $B_q(q)$ (instead of the cranking value) with one adjustable parameter. Extended life time calculations with microscopical inertias $B_q(q)$ using the Nilsson model will soon be published by the Warsaw group (Sobiczewski et al.).

[1] T. Ledergerber and H.C. Pauli, Nucl. Phys. A207 (1973) 1.
[2] J. Randrup et al., Phys. Rev. C13 (1976) 229.
[3] A. Sobiczewski et al., to be published.
[4] D.R. Inglis, Phys. Rev. 96 (1954) 1059 and 103 (1956) 1786.

6."HOT TOPICS" - SOME OPEN QUESTIONS

We mention here some open problems related to the static barrier picture discussed above and its possible limitations. Rather than presenting a detailed discussion and reproducing many figures, we shall just give some key arguments and refer to the relevant literature.

6.1. Th-anomaly: triple-humped barriers?

We have already mentioned (in sect. 5.3) the so-called Th-anomaly and a possible interpretation in terms of a triple-humped barrier [MN73]. If this interpretation is correct, one has to consider other possible consequences of the existence of a third minimum. In a recent experiment at Saclay[1], a shape-vibrational resonance in the fission of the Th^{233} compound-nucleus was investigated with high resolution. Some fine structures with rotational band-like nature were observed. The corresponding moments of inertia are larger than the typical values found in the second wells of Pu^{240} and U^{236} (see sect. 5.4.b) and would be compatible with the deformation of the second saddle point, if one interpolates between the values of the neighbouring even-A isotopes. However, in Th^{233}, the blocking effect of the odd neutron has to be taken into account which will give larger moments of inertia, also in the case of rotational bands built on quasiparticle states in the usual second well. Thus, the values of $\mathcal{J}$ do not prove the existence of a third minimum.

A recent analysis of photo-fission data on Th^{232} [2] seems to favour the usual double-humped barrier with the second minimum at $\sim$ 3 MeV (and not one at $\sim$4.5 MeV).

If the usual double-humped barrier picture is to be maintained in the lighter neutron-poor actinides, one has to explain why the calculated inner barriers are several MeV too low. It is possible that this defect is related to the "Pb-anomaly", which we attributed (in sect. 5.5) to the missing self-consistency between the LDM energies and the average potentials used in the SCM calculations.

6.2. Superheavy Elements?

Already since the first successes of the SCM, one has speculated about the possibility, that an "island" of stable nuclei exists with $Z \sim 114\text{-}126$ and $A \sim 300\text{-}350$. Although the LDM part of the deformation energy does not give a stable ground state for such nuclei ($X \lesssim 50$), a sufficiently strong shell effect (preferably at the spherically magic numbers $Z = 114$; $N = 184, 226$) might produce a barrier which is high enough to lead to an experimentally detectable fission lifetime. Indeed, barriers of $\sim$7-12 MeV were obtained in the calculations for such nuclei. However, the main problem is here the unreliability of extrapolating LDM and shell model potential parameters to unknown regions. Indeed, the different models and parameter sets give differences of several MeV in the predicted barrier heights (which means ten or more orders of magnitude uncertainty in the life times!). We refer to conference reports for details of these calculations (Ronneby, 1974 and ref.[1]).

The use of the HF method with effective interactions might be more reliable for such extrapolations, since relatively few parameters ($\sim$7) are used here which are the same for all known nuclei from $A \sim 16$ to $A \sim 250$. But the constrained HF calculations are too time consuming - at least at the moment - for systematic studies for these superheavy nuclei, so that further approximations are necessary which lead to further uncertainties.

As to the experimental searches for "superheavies", both in nature and in the laboratory (heavy-ion accelerators), which all have been negative so far, we also refer to the above-mentioned proceedings.

6.3. Fragment mass and kinetic energy distributions

We saw in section 5.2 that already at the second saddle, a preference for mass-asymmetric shapes exists due to the shell effects in the deformation energy. Although this is certainly connected to the asymmetric fragment masses, we cannot explain the mass distributions knowing the potential energy only. One should expect that dynamics play an essential role in the determination of the fragment distributions.

Therefore, it is rather astonishing that it is still possible to explain the qualitative features of the fragment distributions reasonably well without doing dynamical calculations. We shall not discuss here the statistical model of Fong[2] which is known since more than two decades. We will, however, quickly mention the so-called static scission point models used in connection with the Strutinsky SCM[3,4,5]. Here the scission configuration is described by two fragments (so far usually rotational ellipsoids) kept at a finite distance d (which is the distance between the closest points of the two surfaces). The total potential energy of this configuration, $V(N_1,Z_1, N_2,Z_2,\beta_1,\beta_2,d)$, is calculated including interaction and shell-correction energies. Based on the arguments of Nörenberg[6] one assumes a partial equilibrium between collective degrees of freedom (here mainly the asymmetry determined by the nuclear numbers N_iZ_i and the deformations β_i) and negligible coupling between collective and intrinsic degrees (in constrast to the model of Fong, where total statistical equilibrium is assumed, also between collective and intrinsic degrees). The probability for a certain fragment distribution is then given either by a Boltzmann factor[4] $\exp[-V(Z_i,N_i,\beta_i)/T_{coll}]$ where the collective temperature T_{coll} is an adjustable parameter, or - which thermodynamically is probably more correct - by minimizing the free energy[5]. In either case, the fragment distributions are determined by the static potential energy at scission (plus the assumed partial statistical equilibrium).

[1] J. Blons et al., Phys. Rev. Lett. 35 (1975) 1749. The experiment was redone at Geel with even better resolution; the rotational structures seem to be confirmed (J. Blons et al., to be published).

[2] M. Asghar, Z. Physik (in print).

[1] Proceedings of International Symposium on Superheavy Elements, Lubbock, Texas, March 9-11, 1978.

[2] P. Fong, Statistical Theory of Nuclear Fission, Gordon and Breach, N.Y., 1969; see also Phys. Rev. C16 (1977) 251 for recent references.

[3] F. Dickmann and K. Dietrich, Nucl. Phys. A129 (1969) 241.

[4] B.D. Wilkins et al., Phys. Rev. C14 (1976) 229.

[5] M. Prakash et al., Nucl. & Solid State Physics Symp. (India) 19B (1976) 127.

[6] W. Nörenberg, Rochester 1973, Vol. I, p.547 and Vienna 1969, p.51.

Such calculations reproduce many features of fragment mass and kinetic energy distributions, including shell effects, in a qualitative and in some cases even semiquantitative way (see especially the extended calculations of ref.[4] above). Clearly, all the shell effects, which play an essential role in these distributions for low-energy fission, are determined by the shells in the fragments at the scission point, in particular also the asymmetry of the mass distribution (where it occurs). Above in section 5.2 we saw that the most probable mass ratio is also coming out as the result of a shell effect in the parent nucleus at the outer saddle. Thus, the asymmetric mass split seems to be affected very little during the descent from the saddle to the scission point. This was indeed confirmed in approximate dynamical calculations using the two centre model[1]. It was found there that at least the gross features of the mass distribution are mainly determined by the potential energy surface.

The success of the static scission point model makes it worth while investigating somewhat more its theoretical justification. In particular, the choice of the constant distance d has to be justified. The underlying assumption of the presence of a scission barrier must be checked and its dependence on the shape parametrization of the fragments must be investigated. Also, in a more rigorous thermodynamical treatment, the collective temperature T_{coll} and the intrinsic temperature τ_{int} given to the fragments are not free parameters, but should be determined by the total energy balance of the system. Some promising work along these lines is under way[2].

It is interesting to note that many of the features of the fragments can be understood from purely static and statistic considerations at the scission point. The fissioning system seems to have lost most of its memory of what happened between the saddle and the scission point, except for the establishment of the partial equilibrium.

6.4. The role of dynamics

After the above discussion, one cannot withhold any longer the obvious question: where and how do the dynamical aspects come in at all? Certainly they must play a role in the descent between the saddle and the scission point. But the qualitative success of the static scission point model puts at least some boundaries on this role. In particular, it seems to confirm the underlying assumption of this model that the fragments have a negligible pre-scission kinetic energy at the moment of the rupture of the neck. Recent measurements of long range α-particle emission in the fission of U^{236} and Cf^{252} and their analysis[3] also seem to confirm the assumption of a small pre-scission kinetic energy ($\lesssim$5 - 10 MeV). This is in contradiction with dynamical liquid-drop calculations[4] which predict this energy to be larger and to increase with increasing mass number ($\sim$20 - 50 MeV for actinides).

The dissipation during the descent from the saddle must be small enough not to destroy the superfluidity of the lighter actinides, where the preference for the formation of fragments with even Z is a well-known experimental fact[1] (for low-energy fission).

At this point we would have to enter into a discussion of dynamical theories, of the question: one-body or two-body viscosity, etc., which goes beyond the boundaries of our lectures. But this is the field where most theoretical work must be done in the near future. We conclude by referring to a recent article[2] in which both macroscopic and microscopic dynamical models and dissipation mechanisms are discussed and many references to the recent literature can be found.

ACKNOWLEDGEMENT

I am indebted to M. Asghar, C. Guet and H. Nifenecker for many illuminating discussions on the present experimental situation.

LITERATURE

Schools and Conferences

Hirschegg 1974: Second International Workshop on Gross Properties of Nuclei and Nuclear Excitations, Hirschegg (Austria) 1974 (Technische Hochschule Darmstadt, 1974)

Munich 1973: International Conference on Nuclear Physics (Eds. J. de Boer and H.J.Mang, North-Holland, 1973)

Paris 1975 Fifth International Conference on Atomic Masses and Fundamental Constants (Eds. J.H.Sanders and A.H.Wapstra, Plenum Press, 1976)

Rochester 1973 Physics and Chemistry of Fission 1973 (IAEA Vienna 1974)

Ronneby 1974 Nobel Symposium 27 on Superheavy Elements; Proceedings published in Physica Scripta 10A (1974)

Trieste 1971 The Structure of Nuclei, Trieste Lectures 1971 (IAEA Vienna 1972)

Trieste 1975 International Conference on Nuclear Self-Consistent Fields, ICTP Trieste 1975 (Eds. G.Ripka and M.Porneuf, North-Holland, 1975)

[1] J.A. Maruhn and W. Greiner, Phys. Rev. C13 (1976) 2404.
[2] M. Prakash et al., Preprint Bombay (1978), and ref. [5] above.
[3] C. Guet et al., submitted to Journ. de Physique, Lettres (1978), and references therein.
[4] J.R. Nix, Nucl. Phys. A130 (1969) 241.

[1] See e.g. R. Brissot et al., Nucl. Phys. A282 (1977) 109 and references therein.
[2] J.W. Negele et al., Phys. Rev. C17 (1978) 1098.

Varenna 1965 Many-Body Description of Nuclear Structure and Reactions, Varenna Lectures 1965 (Academic Press, 1966)

Vienna 1963 Second International Conference on Nuclidic Masses (Ed. W.H.Johnston Jr., Springer, 1963)

Vienna 1969 Physics and Chemistry of Fission 1969 (IAEA Vienna, 1969)

Books

E.K. Hyde: Nuclear Properties of the Heavy Elements, Vol. III: Fission Phenomena, Prentice-Hall, 1964.

L. Wilets: Theories of Nuclear Fission, Clarendon Press, Oxford, 1964.

R. Vandenbosch and J.R. Huizenga: Nuclear Fission, Academic Press, New York and London, 1973.

M. Preston and R.K. Bhaduri: Structure of the Nucleus, Addison-Wesley, 1975.

AD 72 B.L.Andersen, F.Dickmann and K.Dietrich, Nucl.Phys. A159 (1972) 337

AS 68 M.Abramowitz and I.A.Stegun, Handbook of Mathematical Functions (Dover, N.Y., 1968)

Ba 63 M.Baranger, Cargèse Lectures in Theoretical Physics, 1962 (W.A.Benjamin, New York, 1963)

BB 36 H.A.Bethe and F.Bacher, Rev.Mod.Phys. 8 (1936) 82

BB 68 K.A.Brückner, J.R.Buchler, S.Jorna and R.J.Lombard, Phys.Rev. 171 (1968) 1188

BB 70 R.Balian and C.Bloch, Ann. Phys. (N.Y.) 60 (1970) 401

BB 71 " " " " " 64 (1971) 271

BB 71a " " " " " 63 (1971) 592

BB 72 " " " " " 69 (1972) 76

BC 76 O.Bohigas, X.Campi, H.Krivine and J.Treiner, Phys.Lett. 64B (1976) 381

BD 72 M.Brack, J.Damgaard, H.C.Pauli, A.S.Jensen, V.M.Strutinsky and C.Y. Wong, Rev. Mod. Phys. 44 (1972) 320

BD 73 R.K.Bhaduri and S.DasGupta, Phys.Lett. 47B (1973) 129

Be 37 H.A.Bethe, Rev.Mod.Phys. 9 (1937) 69

Be 68 " Phys.Rev. 167 (1968) 879

Be 71 " Ann.Rev.Nucl.Sci. 21 (1971) 93

Be 72 R.Bengtsson, Nucl.Phys. A198 (1972) 591

Be 73 " Rochester 1973, Vol.I, p. 203

BF 72 M.Bolsterli, E.O.Fiset, J.R.Nix and J.L.Norton, Phys.Rev. C5 (1972) 1050

BF 74 M.Beiner, H.Flocard, N.V.Giai and P.Quentin, Nucl.Phys. A238 (1975) 29; see also M.Beiner, H.Flocard, M.Veneroni and P.Quentin, Ronneby 1974, p.84

BG 58 K.A.Brückner, J.L.Gammel and H.Weitzner, Phys.Rev. 110 (1958) 431

BH 73 B.B.Back, O.Hansen, H.C.Britt, G.D.Garrett and B.Leroux, Rochester 1973, Vol. I, p. 3

Bh 77 R.K.Bhaduri, Phys.Rev.Lett. 39 (1977) 329

BJ 76 G.E.Brown and A.D.Jackson, The Nucleon-Nucleon-Interaction (North-Holland/ Amer.Elsevier, New York, 1976)

BJ 76a M.Brack and B.K.Jennings, Nucl.Phys. A258 (1976) 264

BJ 76b " " and Y.H.Chu, Phys.Lett. 65B (1976) 1

BK 37 N.Bohr and F.Kalckar, Kgl.Dan.Vid.Selsk., Mat.-Fys.Medd. 14 (1937) No. 10

BK 72a G.G.Bunatian, V.M.Kolomietz and V.M.Strutinsky, Nucl.Phys. A188 (1972) 225

BK 72b W.H.Bassichis, A.K.Kerman, C.F.Tsang, D.R.Tuerpe and L.Wilets, "Magic without magics: John Archibald Wheeler" (Freeman, San Francisco, 1972)

BK 73 W.H.Bassichis, A.K.Kerman and D.R.Tuerpe, Phys.Rev. C8 (1973) 2140

BL 74 M.Brack, T.Ledergerber, H.C.Pauli and A.S.Jensen, Nucl.Phys. A234 (1974)185

BL 75 R.Bengtsson, S.E.Larsson, G.Leander, P.Möller, S.G.Nilsson, S.Åberg and Z.Szymanski, Phys.Lett. 57B (1975) 301

BM 55 A.Bohr and B.Mottelson, Kgl.Dan.Vid.Selsk., Mat.-Fys.Medd. 30 (1955) No. 1

BM 69 " " Nuclear Structure, Vol. I (Benjamin, 1969)

BM 75 A.Bohr and B.Mottelson, Nuclear Structure, Vol. II (Reading, 1975)

Bo 57 N.N.Bogolyubov et al., Doklady (Sovjet Phys.) 2 (1957) 535

BP 73 M.Brack and H.C.Pauli; Nucl.Phys. A207 (1973) 401

BP 77a J.Borggreen, J.Pedersen, G.Sletten, R.Heffner and E.Swanson, Nucl.Phys. A279 (1977) 189

BP 77b N.Balazs and H.C.Pauli, Preprint Heidelberg, 1977

BQ 73 M.Brack and P.Quentin, Rochester 1973, Vol. I, p. 231

BQ 74a " " Ronneby 1974, p. 163

BQ 74b " " Phys.Lett. 52B (1974) 159

BQ 75a " " Trieste 1975, p. 353

BQ 75b " " Phys.Lett. 56B (1975) 421

BQ 75c " " Paris 1975, p. 257

BQ 75d " " Trieste 1975, p. 399

Br 55 K.A.Brückner, Phys.Rev. 97 (1955) 1353

Br 67 B.H.Brandow, Rev.Mod.Phys. 39 (1967) 771

BR 71 R.K.Bhaduri and C.K.Ross, Phys.Rev.Lett. 27 (1971) 606

Br 74a M.Brack, Hirschegg 1974, p. 14

Br 74b " Lectures given at the International School of Nuclear Physics, Predeal (Romania) 1974

Br 76 M.Brack, Seminar given at Orsay, 1976

Br 77 " Phys.Lett. 71B (1977) 239

BS 69 S.Bjørnholm and V.M.Strutinsky, Nucl.Phys.A136 (1969) 1

BW 39 N.Bohr and J.A.Wheeler, Phys.Rev. 56 (1939) 426

BW 55 R.A.Berg and L.Wilets, Proc.Phys.Soc.Lon. A68 (1955) 229

BW 56 " " Phys.Rev. 101 (1956) 201

BW 69 W.H.Bassichis and L.Wilets, Phys.Rev.Lett. 22 (1969) 79

BW 71 " " " " " 27 (1971) 1451

BZ 73 N.Balazs and G.Zipfel, Ann.Phys.(N.Y.) 77 (1973) 139

Ch 77 Y.H.Chu, Doctoral Thesis, Stony Brook, 1977

CJ 77 Y.H.Chu, B.K.Jennings and M.Brack, Phys.Lett. 68B (1977) 407

CP 74 S.Cohen, F.Plasil and W.J.Swiatecki, Ann.Phys.(N.Y.) 82 (1974) 557

CS 63 " and W.J.Swiatecki, Ann.Phys.(N.Y.) 22 (1963) 406

CS 72 X.Campi and D.W.Sprung, Nucl.Phys.A194 (1972) 401

Da 67 B.D.Day, Rev.Mod.Phys. 39 (1967) 719

DB 77 M.Durand, M.Brack and P.Schuck, Preprint ILL Grenoble, 1977

De 68 J.Des Cloiseaux in "Many Body Physics", Les Houches 1967 (Gordon and Breach, New York, 1968)

Di 72 K.Dietrich, Trieste 1971, p. 373

DJ 74 T.Døssing and A.S.Jensen, Nucl.Phys. A222 (1974) 493

DM 73 K.T.R.Davies, R.J.McCarthy and P.U.Sauer, Phys.Rev. C7 (1973) 943

DM 75 M.Dworcecka and S.A.Moszkowski, Phys.Rev. C12 (1975) 619

DP 69a J.Damgaard, H.C.Pauli, V.V.Pashkevich and V.M.Strutinsky, Nucl.Phys. A135 (1969) 432

DP 69b J.Damgaard, H.C.Pauli, V.M.Strutinsky, C.Y.Wong, M.Brack and A.S.Jensen, Vienna 1969, p. 213

DR 74 S.DasGupta and S.Radhakant, Phys.Rev. C9 (1974) 1775

EM 72 D.Ehlers and S.A.Moszkowski, Phys.Rev. C6 (1972) 217

Fl 75 H.Flocard, Trieste 1975, p. 219

Fl 76 " Thèse d'Etat, Orsay, 1976

FQ 73a H.Flocard, P.Quentin, A.K.Kerman and D.Vautherin, Nucl.Phys. A203 (1973) 433

FQ 73b H.Flocard, P.Quentin, D.Vautherin and A.K.Kerman, Rochester 1975, Vol. I, p. 221

FQ 74 H.Flocard, P.Quentin, D.Vautherin, M.Véneroni and A.K.Kerman, Nucl. Phys. A231 (1974) 176

Fr 39 J.A.Frenkel, Zhur.Eksptl. i Teor.Fyz. 9 (1939) 641

GB 57 M.Gell-Mann and K.A.Brückner, Phys.Rev. 106 (1957) 364

GB 77 A.Gavron, H.C.Britt, P.D.Goldstone, J.B.Wilhelmy and S.E.Larsson, Phys.Rev.Lett. 38 (1977) 1457

GM 71 J.Grumann, T.Morovic and W.Greiner, Z.Naturforsch. 26a (1971) 643

Go 48 P.Gombas, Die Statistische Theorie des Atoms, (Springer, Vienna, 1948)

Go 73 D.Gogny, Munich 1973, Vol. I, p. 48

Go 75 " Trieste 1975, p. 333

GP 72 U.Götz, H.C.Pauli, K.Junker and K.Alder, Nucl.Phys. A192 (1972) 1

Gr 72 D.H.E.Gross, Phys.Lett. 42B (1972) 41

GS 69 M.Gaudin and A.M.Sajot, Vienna 1969, p. 229

GS 77 G.Gumpertsberger and P.Schuck; Phys.Lett. 66B (1977) 219

GV 77 B.Grammaticos and A.Voros, private communication, 1977

HJ 49 O.Haxel, J.H.D Jensen and H.E.Suess, Phys.Rev. 75 (1949) 1766

HJ 62 T.Hamada and T.D.Johnston, Nucl.Phys. 34 (1962) 382

HK 64 P.Hohenberg and W.Kohn, Phys.Rev. 136 (1964) B864

HM 72 J.K.Huizenga and L.G.Moretto, Ann.Rev.Nucl.Sci. 22 (1972) 427

HM 77 D.Habs, V.Metag, H.J.Specht and G.Ulfert, Phys.Rev.Lett. 38 (1977) 387

HN 77 P.Hoodbhoy and J.W.Negele, Nucl.Phys. A288 (1977) 23

Ho 73 C.H.Hodges, Can.J.Phys. 51 (1973) 1428

HS 73 R.W.Hasse and W.Stocker, Phys.Lett. 44B (1973) 26

Hu 57 J.Hubbard, Proc.Roy.Soc. (London) A243 (1957) 336

HW 53 D.L.Hill and J.A.Wheeler, Phys.Rev. 89 (1953) 1102

JB 75a B.K.Jennings and R.K.Bhaduri, Nucl.Phys. A237 (1975) 149

JB 75b B.K.Jennings, R.K.Bhaduri and M.Brack, Phys.Rev.Lett. 34 (1975) 228

JB 75c " " " Nucl.Phys. A253 (1975) 29

JD 73 A.S.Jensen and J.Damgaard, Nucl.Phys. A203 (1973) 578

Je 73 B.K.Jennings, Nucl.Phys. A207 (1973) 538

Je 74 " Ann.Phys. (N.Y.) 84 (1974) 1

Je 76 " Ph.D. Thesis, McMaster University, 1976

JH 77 K.Junker and J.Hadermann, Z.Physik A282 (1977) 391

JN 70 T.Johansson, S.G.Nilsson and Z.Szymanski, Ann.Phys. (Paris) 5 (1970) 377

Ju 74 K.Junker, Atomkernenergie (ATKE) Vol. 23 (1974) 57

Ju 75 " Acta Phys. Austr. 43 (1975) 221

KB 61 K.Kumar and R.K.Bhaduri, Phys.Rev. 122 (1961) 1926

KC 73 D.Kolb, R.Y.Cusson and M.Harvey, Nucl.Phys. A215 (1973) 1

Ki 33 J.G.Kirkwood, Phys.Rev. 44 (1933) 31

Ki 57 D.A.Kirzhnits, Sovj.Phys. JETP 5 (1957) 64

Ko 73 V.M.Kolomietz, Yad.Fiz. 18 (1973) 288 [Sov.J.Nucl.Phys. 18 (1974) 147]

KP 73 C.M.Ko, H.C.Pauli, M.Brack and G.E.Brown, Phys.Lett. 45B (1973) 433

KP 74 " " " " Nucl.Phys. A236 (1974) 269

KR 69 P.B.Kahn and R.Rosenzweig, Phys.Rev. 187 (1969) 1193

KS 65 W.Kohn and L.J.Sham, Phys.Rev. 137 (1965) A1697; ibid. 140 (1965) A1133

KW 72 S.J.Krieger and C.Y.Wong, Phys.Rev.Lett. 28 (1972) 690

La 37 R.E.Langer, Phys.Rev. 51 (1937) 669

La 64 A.M.Lane, Nuclear Theory (Benjamin, New York, 1964)

LL 74 S.E.Larsson, G.Leander, I.Ragnarsson and J.Randrup, Ronneby 1974, p. 65

LL 75 S.E.Larsson and G.Leander, Nucl.Phys. A239 (1975) 93

Lo 73 R.J.Lombard, Ann.Phys. (N.Y.) 77 (1973) 380

Ma 49 M.G.Mayer, Phys.Rev. 75 (1949) 1969

Ma 77 R.S.Mackintosh, Rep. Prog. Phys. 40 (1977) 731

MG 53 S.C.Miller Jr. and R.H.Good, Phys.Rev. 91 (1953) 174

Mi 67 A.B.Migdal, Theory of finite Fermi systems and properties of atomic nuclei (Moscow, 1965; Interscience, New York, 1967)

MM 73 M.G.Mustafa, U.Mosel and H.W.Schmitt, Phys.Rev. C7 (1973) 1519

MN 70 P.Möller and S.G.Nilsson, Phys.Lett. 31B (1970) 283

MN 73 P.Möller and J.R.Nix, Rochester 1973, Vol. I, p. 103; see also Nucl. Phys. A229 (1974) 269

Mo 70 S.A.Moszkowski, Phys.Rev. C2 (1970) 402

Mo 72 L.G.Moretto, Phys.Lett. 38B (1972) 393

Mö 72 P.Möller, Nucl.Phys. A192 (1972) 529

MS 66 W.D.Myers and W.J.Swiatecki, Nucl.Phys. 81 (1966) 1

MS 69 " " Ann.Phys. (N.Y.) 55 (1969) 395

MS 70 L.G.Moretto and R.Stella, Phys.Lett. 32B (1970) 558

MS 77 V.Metag and G.Sletten, Nucl.Phys. A282 (1977) 77

My 69 W.D.Myers, Nucl.Phys. A145 (1969) 387

MZ 74 U.Mosel, P.Zint and K.Passler, Nucl.Phys. A236 (1974) 252

Ne 70 J.W.Negele, Phys.Rev. C1 (1970) 1260

Ne 75 " Trieste 1975, p. 113

Ni 55 S.G.Nilsson, Kgl.Dan.Vid.Selsk., Mat.-Fys.Medd. 29 (1955) No. 16

Ni 69 J.R.Nix, Nucl.Phys. A130 (1969) 241

Ni 72 " Ann.Rev.Nucl.Sci. 22 (1972) 65

NP 58 P.Nozières and D.Pines, Phys.Rev. 111 (1958) 442

NT 69 S.G.Nilsson, C.F.Tsang, A.Sobiczewski, Z.Szymanski, S.Wychec, C.Gustafsson, I.L.Lamm, P.Möller and B.Nilsson, Nucl.Phys. A131 (1969) 1

NV 70 J.Nemeth and D.Vautherin, Phys.Lett. 32B (1970) 561

NV 72 J.W.Negele and D.Vautherin, Phys.Rev. C5 (1972) 1472

NV 75 " " " " C11 (1975) 1031

OZ 77 S.R.Ofengenden, V.F.Zavarzin and V.M.Kolomietz, Phys.Lett. 69B (1977) 264

Pa 73 H.C.Pauli, Phys.Reports (Phys.Lett.C) 7 (1973) 35

PL 71 H.C.Pauli, T.Ledergerber and M.Brack, Phys.Lett. 34B (1971) 264

PL 73 " and T.Ledergerber, Rochester 1973, Vol. I, p. 463

Po 62 S.Polikanov et al., JETP (Sov.Phys.) 15 (1962) 1016

Qu 75a P.Quentin, Trieste 1975, p. 297

Qu 75b " Thèse d'Etat, Orsay, 1975

RB 72 C.K.Ross and R.K.Bhaduri, Nucl.Phys. A188 (1972) 566

Re 68 R.V.Reid, Ann.Phys. (N.Y.) 50 (1968) 411

RK 72 V.S.Ramamurthy and S.S.Kapoor, Phys.Lett. 42B (1972) 399

Sa 75 P.U.Sauer, Trieste 1975, p. 89

SB 73 W.Stocker and J.Burzlaff, Nucl.Phys. A202 (1973) 265

SB 77 V.M.Strutinsky, private communication; M.Brack, unpublished results (1977)

SC 76 G.Sauer, H.Chandra and U.Mosel, Nucl.Phys. A264 (1976) 221

SG 71 D.Scharnweber, W.Greiner and U.Mosel, Nucl.Phys. A164 (1971) 275

SG 77 A.Sobiczewski, A.Gyurkovich and M.Brack, Nucl.Phys. A289 (1977) 346

SI 75 V.M.Strutinsky and F.A.Ivanjuk, Nucl.Phys. A255 (1975) 405

Sk 57 T.H.R.Skyrme, Proc.Phys.Soc. A70 (1957) 433

Sk 56 " Phil.Mag. 1 (1956) 1043

Sk 59 " Nucl.Phys. 9 (1959) 615

SL 63 V.M.Strutinsky, N.Ljashchenko and N.A.Popov, Nucl.Phys. 46 (1963) 639

SM 72 H.W.Scmitt and U.Mosel, Nucl.Phys. A186 (1972) 1

SM 77 V.M.Strutinsky, A.G.Magner, S.R.Ofengenden and T.Døssing, Z.Physik A283 (1977) 269

Sp 74 H.J.Specht, Rev.Mod.Phys.46 (1974) 773

SS 72 P.J.Siemens and A.Sobiczewski, Phys.Lett. 41B (1972) 16

St 66 V.M.Strutinsky, Yad.Fiz. 3 (1966) 614 [Sov.J.Nucl.Phys. 3 (1969) 449]

St 67 " Nucl.Phys. A95 (1967) 420

St 68 " " " A122 (1968) 1

St 74 V.M.Strutinsky, Nucl.Phys. A218 (1974) 169

St 75 " " " A254 (1975) 197

Sw 55 W.J.Swiatecki, Proc.Phys.Soc. A65 (1955) 285

SW 72 H.J.Specht, J.Weber, E.Konecny and D.Heunemann, Phys.Lett. 41B (1972) 43

SY 63 M.Sano and S.Yamasaki, Progr.Theor.Phys. 29 (1963) 397

Ta 64 F.Tabakin, Ann.Phys. (N.Y.) 30 (1964) 51

Ts 69 C.F.Tsang, Ph.D. Thesis, Berkeley, 1969
Ty 70 A.S.Tyapin, Sov.J.Nucl.Phys. 11 (1970) 401
Ty 72 " " " " 14 (1972) 50
UB 36 G.E.Uhlenbeck and E.Beth, Physica 3 (1936) 729
Va 69 D.Vautherin, Thèse d'Etat, Orsay, 1969
Va 73 " Phys.Rev. C7 (1973) 296
VB 72 " and D.Brink, Phys.Rev. C5 (1972) 626
Vo 77 A.Voros, Thèse d'Etat, Saclay, 1977
WC 72 F.C.Williams, G.Chan and J.R.Huizenga, Nucl.Phys. A187 (1972) 225
We 35 C.F.v.Weizsäcker, Z.Physik 96 (1935) 431
Wi 32 E.P.Wigner, Phys.Rev. 40 (1932) 749
Wi 34 " Phys.Rev. 40 (1934) 1002
Wi 58 L.Wilets, Rev.Mod.Phys. 30 (1958) 542
Wi 69 " Vienna 1969, p. 179
Yu 35 H.Yukawa, Proc.Phys.-Math.Soc.,Japan 17 (1935) 48

Table 1.1 Comparison of theoretical LDM barriers (E_{th}) and measured barriers (E_{exp}), both in MeV. Values of X calculated with $(Z^2/A)_{crit} = 50$. (From Wilets, 1964).

Nucleus	X	E_{th}	E_{exp}
Th^{233}	0.694	15.58	6.44
Th^{232}	0.697	15.08	5.95
U^{239}	0.707	13.51	6.15
U^{238}	0.710	13.06	5.80
Ra^{232}	0.713	12.68	6.18
U^{237}	0.713	12.63	6.40
U^{235}	0.719	11.79	5.75
U^{233}	0.725	10.96	5.49
Np^{238}	0.725	10.92	6.04
Np^{237}	0.729	10.53	5.49
Pu^{239}	0.738	9.39	5.48

FIGURE CAPTIONS

Fig. 1.1: LDM energy surface as function of a_{20} and a_{40} deformations for a nucleus with $x = 0.8$. Equidistance of contour lines in units of the surface energy $E_{surf}(0)$. (From Wilets, 1964).

Fig. 1.2: Nilsson levels for protons, $82 < Z < 126$. (From Vandenbosch and Huizenga, 1973).

Fig. 2.1: Fission barrier of Pu^{240} obtained with a constrained HF calculation with the force Skyrme III [FQ 736]. Dashed and solid lines correspond to different ways of including pairing. Dots (with arrows) give the energies (and slopes of the curve) at the two minima and the 2. saddle when the basis is increased (to demonstrate convergence). For details see [FQ 74].

Fig. 3.1: Exact HF energy (E_{HF}) and its average part ($\bar{E}$; $\tilde{E}_{HF}$ in the text above) obtained with force Sky III. E_{LD} shows the LDM energy (adjusted at $Q_2 \simeq 0$) obtained with the parameters of [MS 66].

Fig. 3.2: Same as Fig. 3.1 with force Negele - DME.

Fig. 3.3: Shell-corrections δE_1 and δE_2 corresponding to the two previous figures, and δE_1 from usual WS potential [BD 72] for comparison.

Fig. 3.4: Values of δE_2 for various nuclei in their ground-states.

Fig. 3.5: As in Fig. 3.1, but here $\tilde{E}$ is calculated selfconsistently.

Fig. 4.1: Axially symmetric shapes as functions of elongation (c) and necking (h) parameters. The shapes along $h = 0$ correspond to the LDM fission valley in a typical actinide nucleus. The dotted curves include some left/right asymmetry ($\alpha \neq 0$) typical at the second saddle ($c \sim 1.6$) [Pa 73].

Fig. 4.2: Neutron levels ε_i^n of the Pu^{240} ($N = 146$) obtained with the deformed Woods-Saxon potential [BD 72, PA 73] versus elongation c ($n = \alpha = 0$). Numbers in circles show "magic" numbers (note the deformed shell $n = 146$ at $c \simeq 1.4$ which leads to the shape isomer in Pu^{240}!). Odd parity states are dotted; the numbers inserted correspond to twice the K value (projection of ang. momentum along symmetry axis).

Fig. 4.3 Density of single-particle states g(E) in Pu^{240} at different deformations c ($h = \alpha = 0$). At the top, some nucleon numbers are indicated (magic numbers for $c = 1$). The dashed lines represent the uniform level density $\tilde{g}(E)$.

Fig. 4.4: Shell-correction δE for a spherical harmonic oscillator well with 70 particles, versus smoothing width γ. The numbers in parentheses are M/2. Note that the length of the plateau increases with the number of levels (shells) included [BP 73].

Fig. 4.5: As in Fig. 4.4, for a spherical Woods-Saxon potential [SG 77]. The inserted plot shows the stationary value $\delta E(\gamma_o)$ according to eq. 4.10 versus order M of curvature correction.

Fig. 4.6: As in Fig. 4.4, for Z = 94 protons in WS potential at different deformations c [BP 73].

Fig. 4.7: Proton levels ε_i^p in deformed WS potential and values of the occupation number differences δn_i in a region $\sim \pm \hbar\omega$ around the Fermi level λ [BP 73].

Fig. 5.1 Deformation energy surface for Pu^{240} for symmetric shapes ($\alpha = \gamma = 0$). Upper right: LDM energy. Left side: proton and neutron shell-corrections δE_p, δE_n (including pairing). Lower right: total energy. Numbers along contour lines show energy in MeV.

Fig. 5.2: Shapes of Pu^{240} nucleus at the four stationary points in the (c,h) surface. Dashed line at second saddle: asymmetry $\alpha \neq 0$ included.

Fig. 5.3: Total energy of Pu^{240} in region including isomer minimum and outer saddle. Upper part: symmetric shapes. Lower part: energy minimized with respect to α in each point (c,h).

Fig. 5.4: Potential energy surface of U^{236} calculated with the two-centre model [MM 73], as function of neck radius D and mass ratio. Energy contours in MeV (relative to g.-s.). The region between ground-state and second minimum (at $\sim$1 MeV) is only indicated partially. The asymmetry reduces the second saddle from 8 to 5.7 MeV.

Fig. 5.5: Comparison of experimental and theoretical barriers of actinide nuclei. The figure includes two newly measured barriers E_A of Pu^{232} and Pu^{234} using β-delayed fission [D. Habs et al., to be published in Z. Physik A, 1968]. I am indebted to H. Specht for providing me with this figure prior to its publication.

Fig. 5.6: Comparison of experimental $\delta M_{exp.}$ (top) and theoretical shell-corrections δM_{th} (middle) to ground-state masses. (Bottom: $\delta M_{exp.} - \delta M_{th}$). From [MN 73].

Fig. 5.7: Potential energy surface of Pu^{240} obtained with WS potential [BD 72]. Upper part: as in Fig. 5.1. Lower part: as function of elongation c and asymmetry α. The solid heavy line is the projection of the least action trajectory onto the corresponding surfaces. Crosses show the locus of constant mass ratio 1.43 of the nascent fragments (from [PL 73]).

Fig. 5.8: Comparison of calculated (dots) and measured (crosses) life times for spontaneous fission. (From [PL 73]).

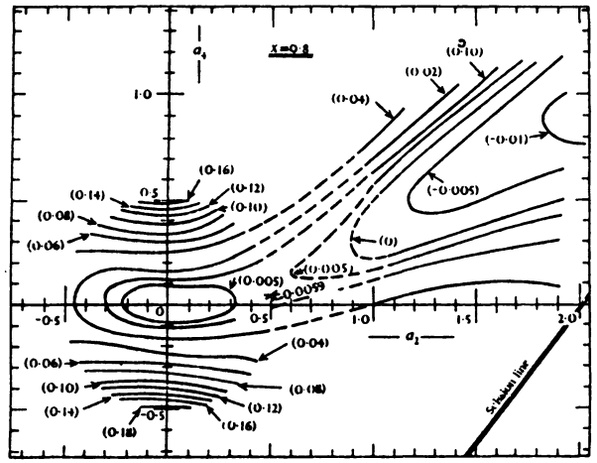

Fig. 1.1

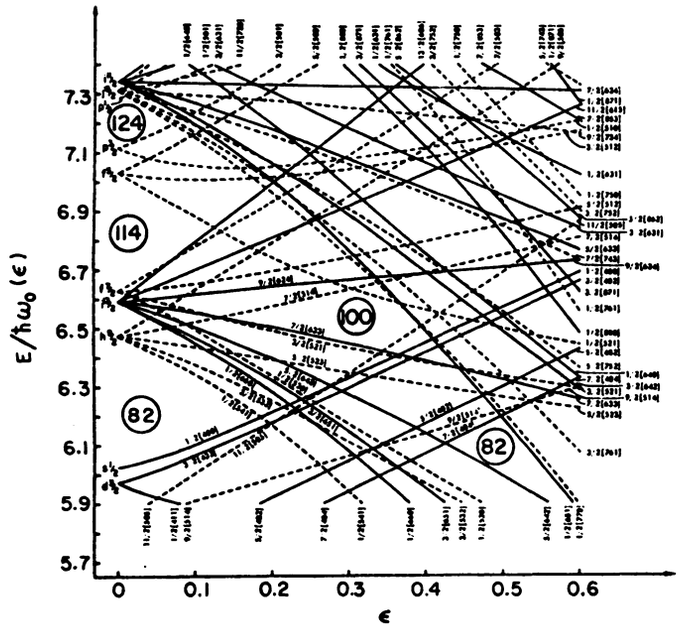

Fig. 1.2

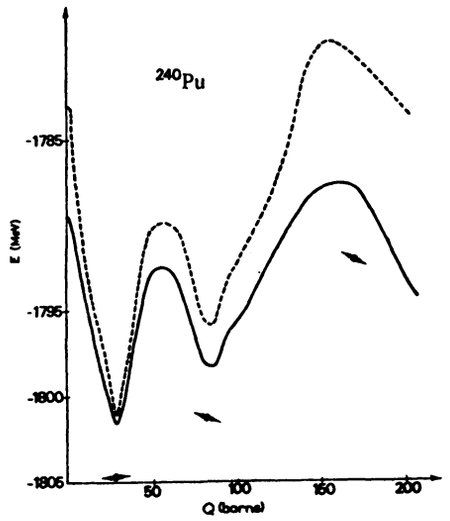

Fig. 2.1

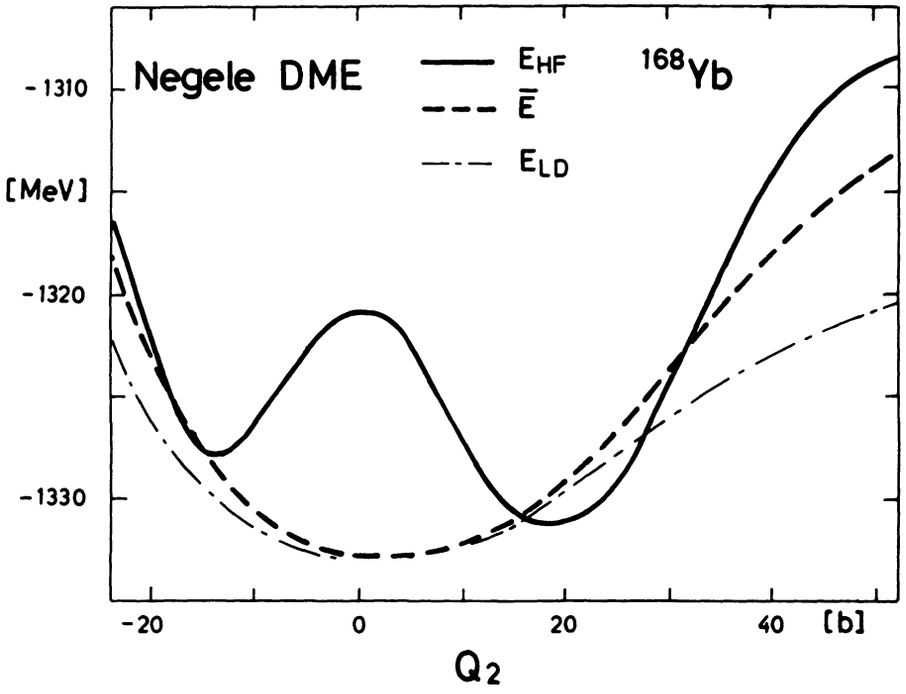

Fig. 3.2

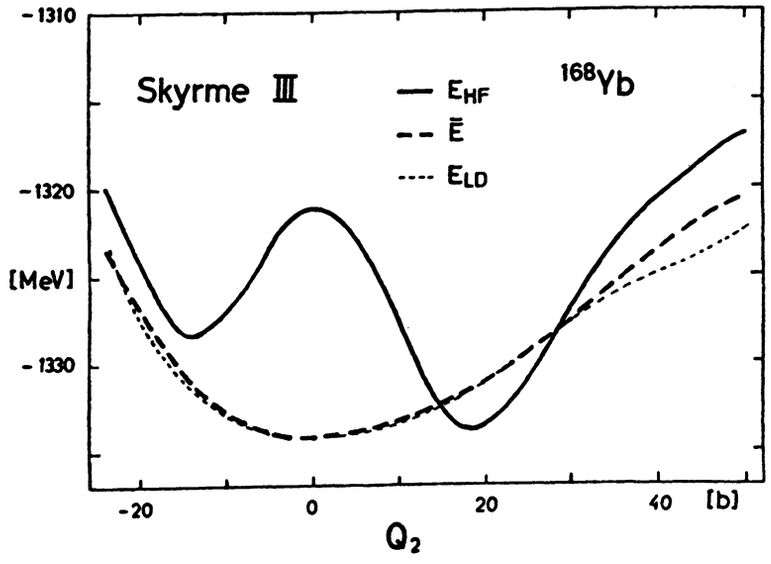

Fig. 3.1

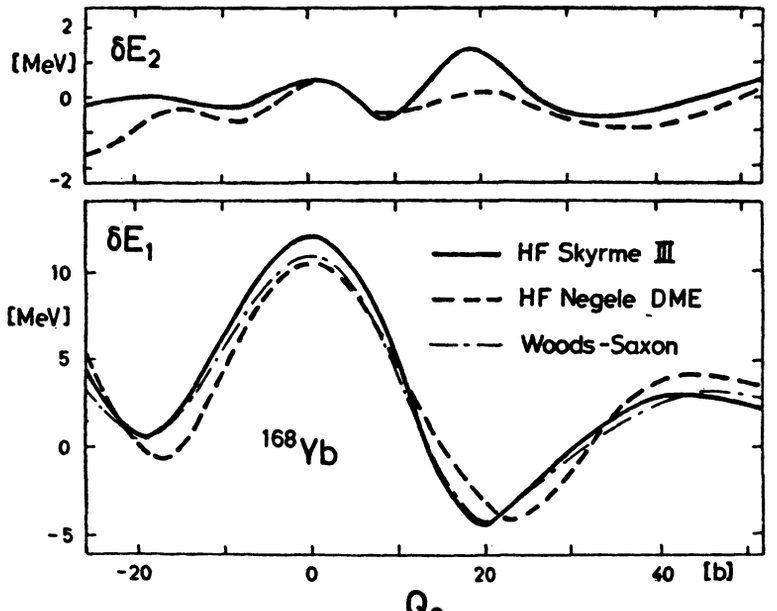

Fig. 3.3

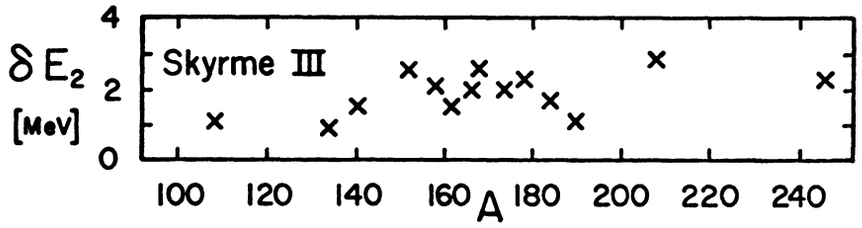

Fig. 3.4

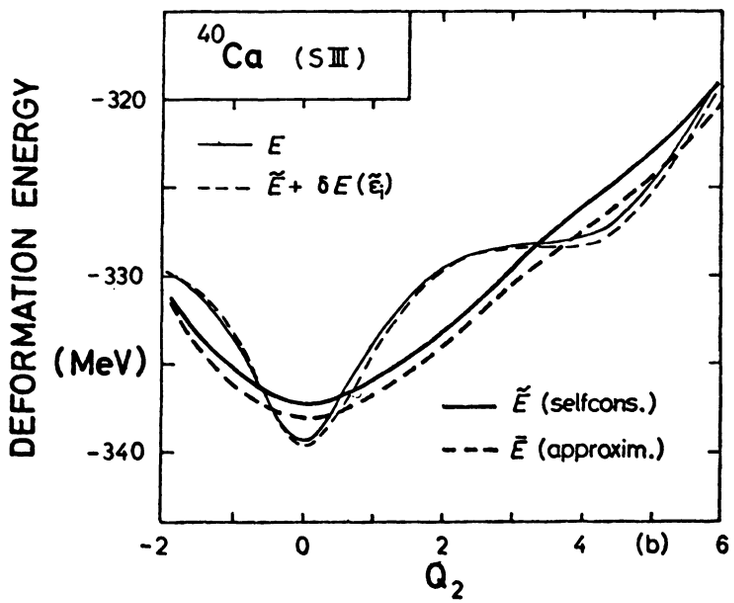

Fig. 3.5

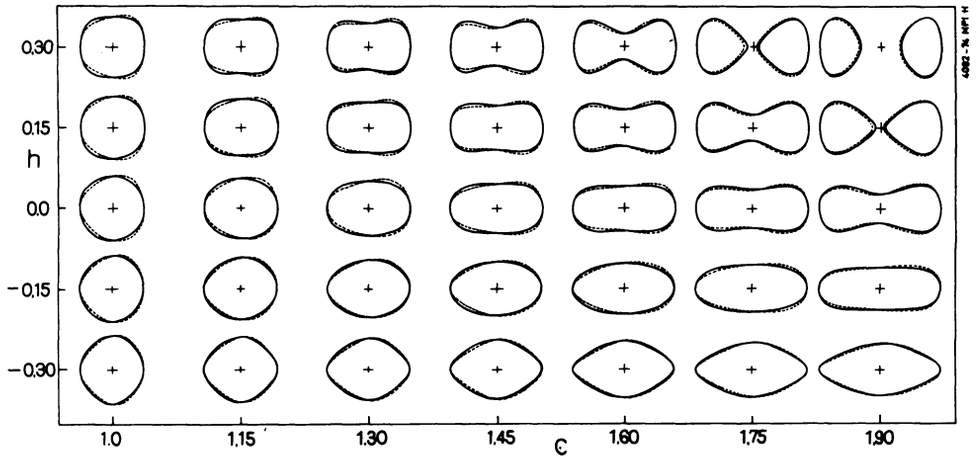

Fig. 4.1

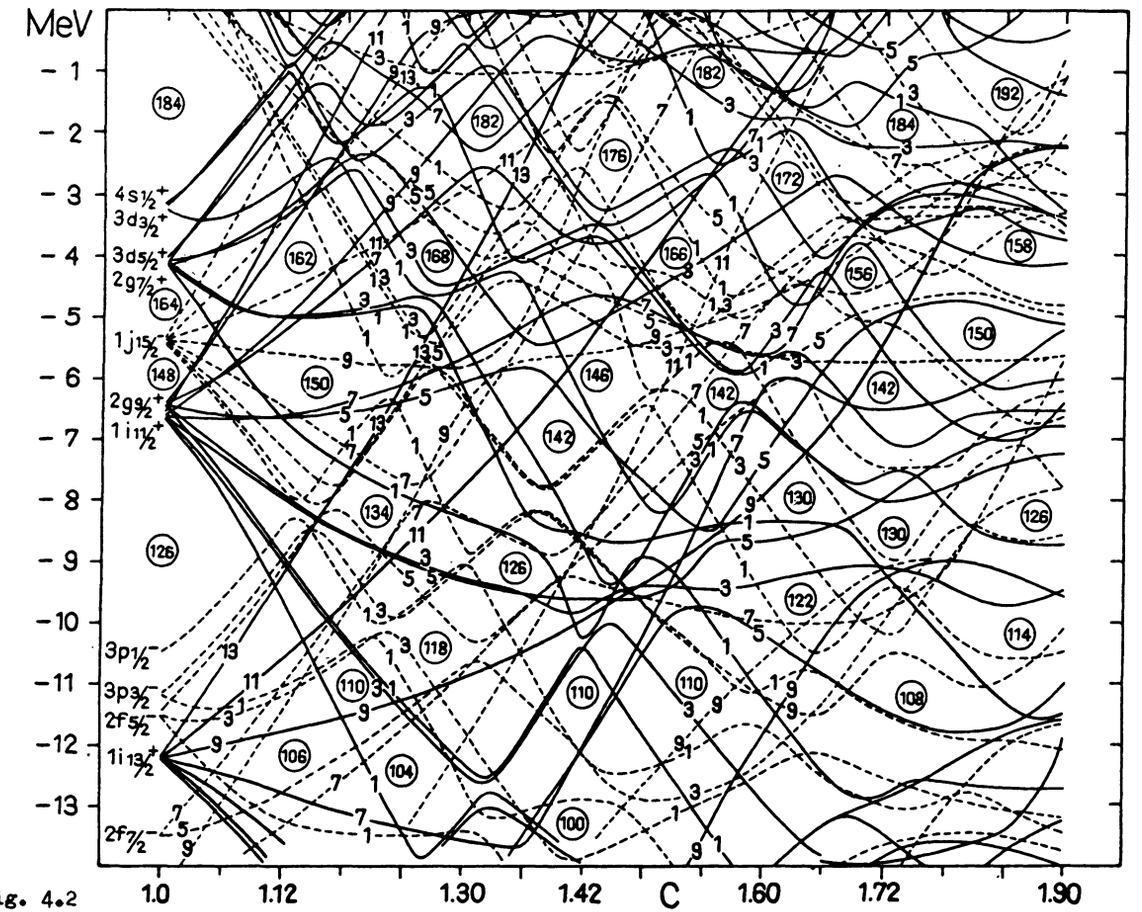

Fig. 4.2

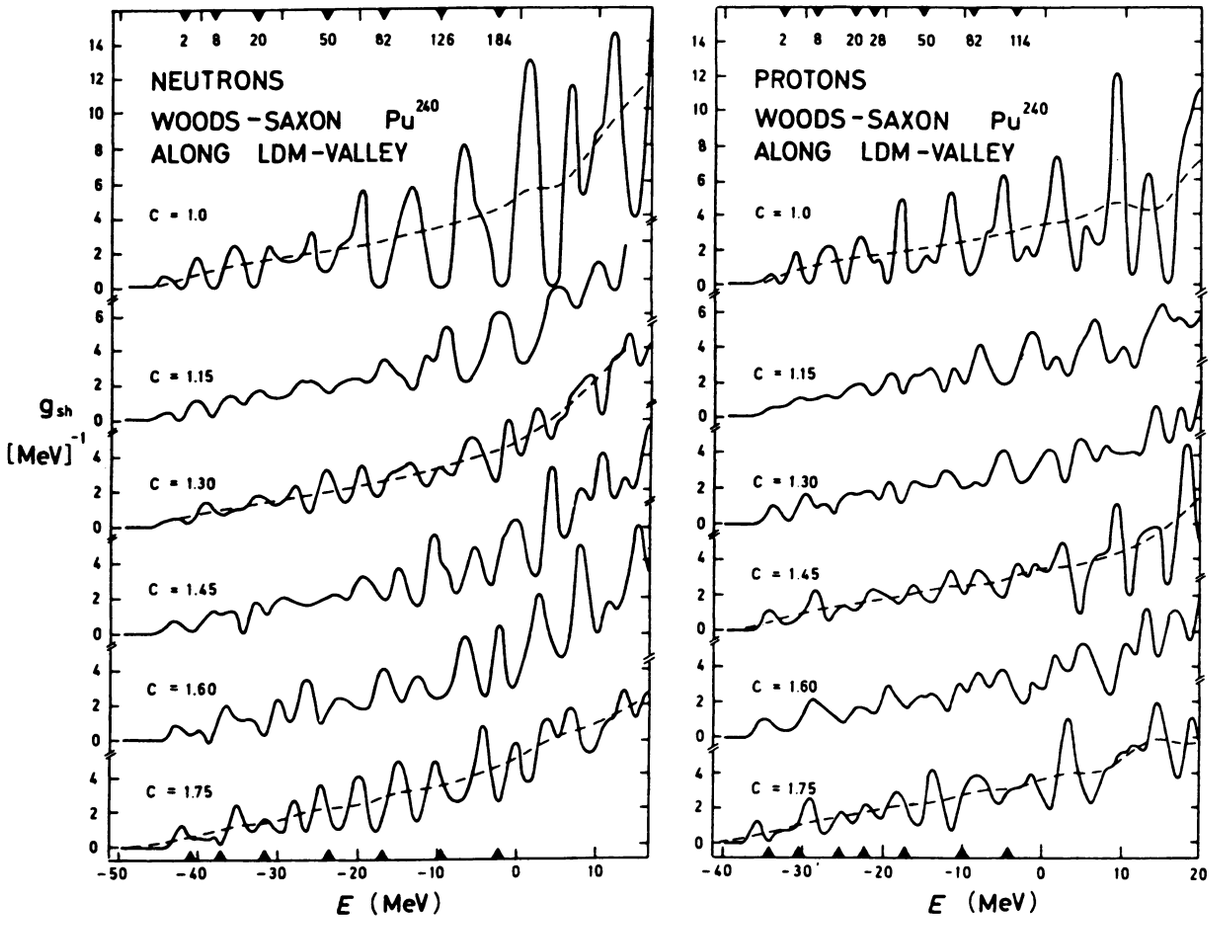

Fig. 4.3

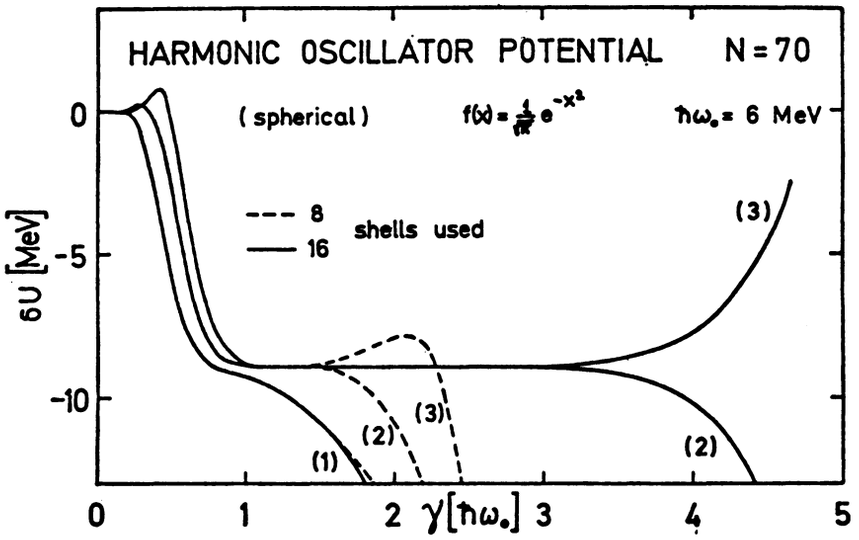

Fig. 4.4

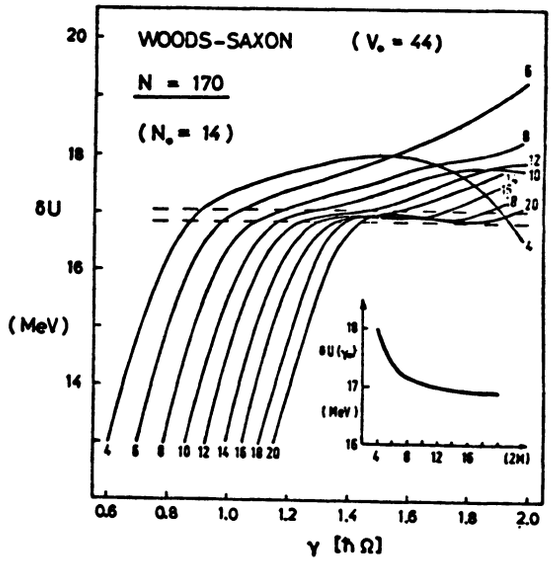

Fig. 4.5

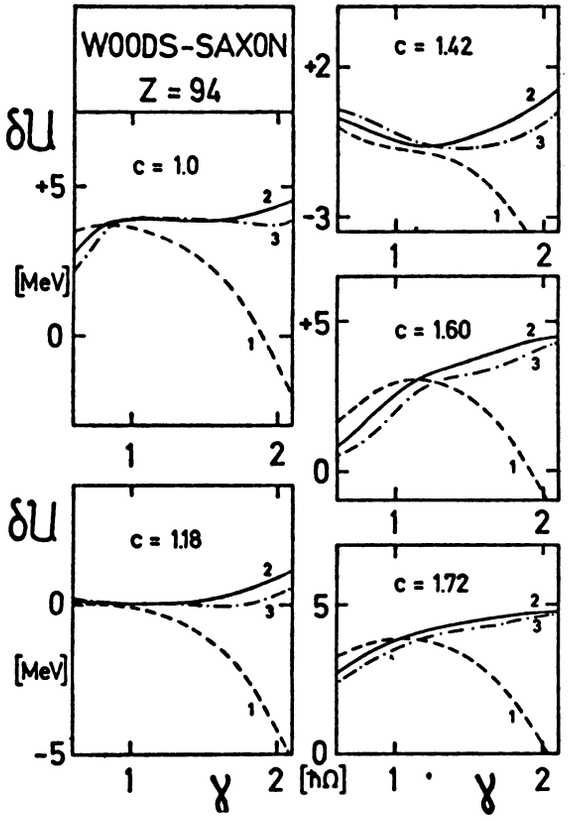

Fig. 4.6

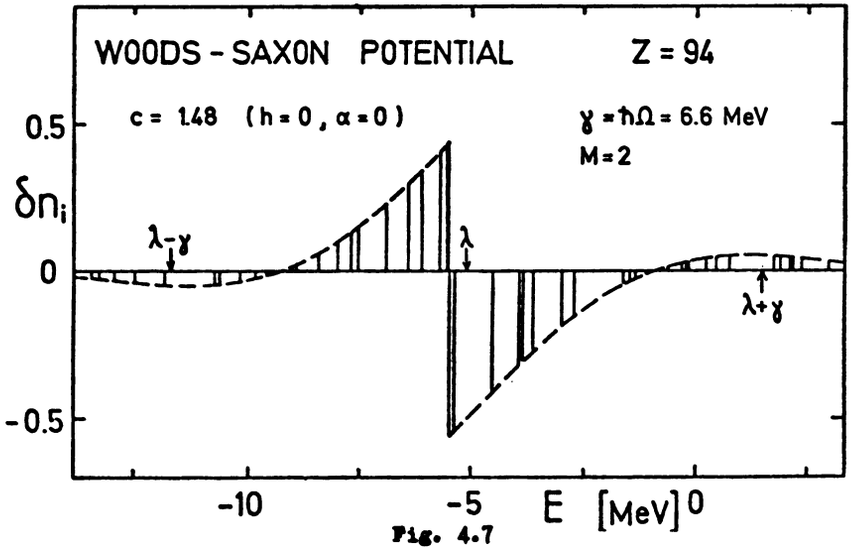

Fig. 4.7

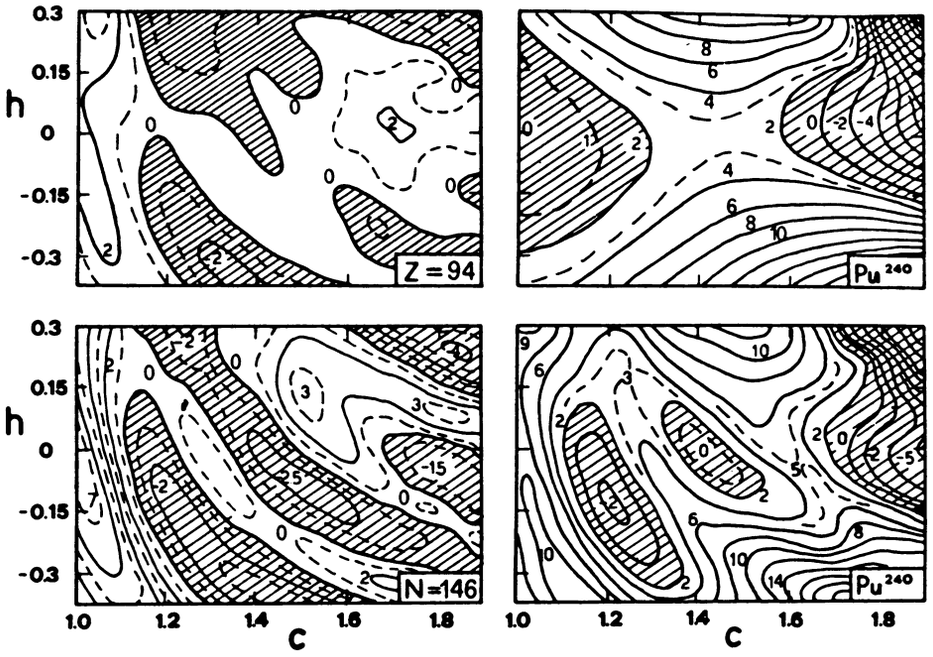

Fig. 5.1

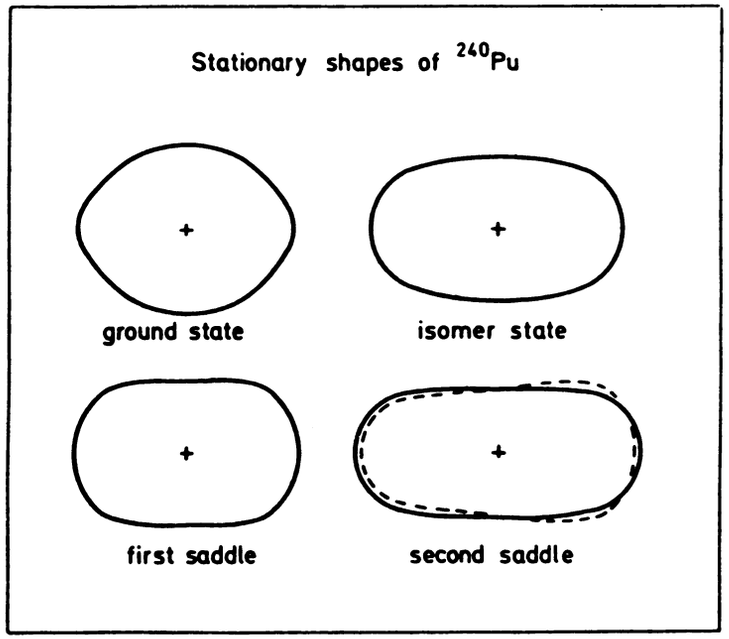

Fig. 5.2

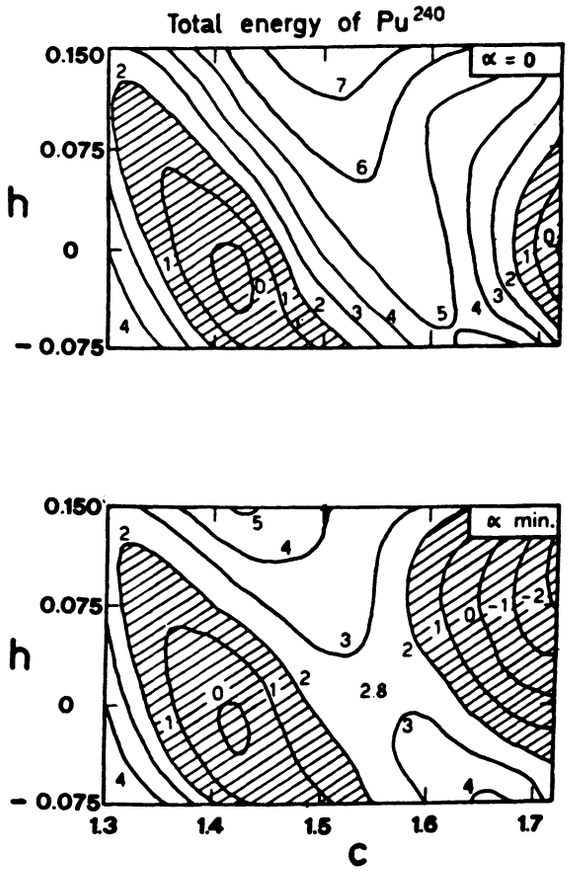

Fig. 5.3

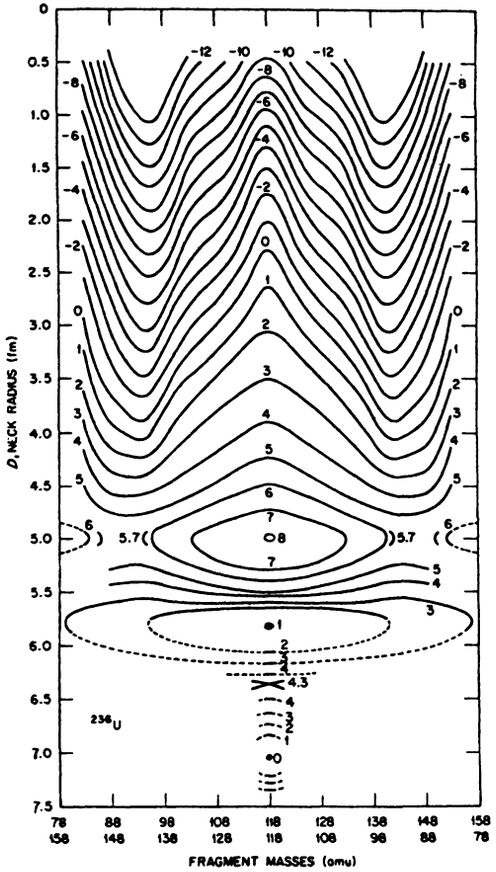

Fig. 5.4

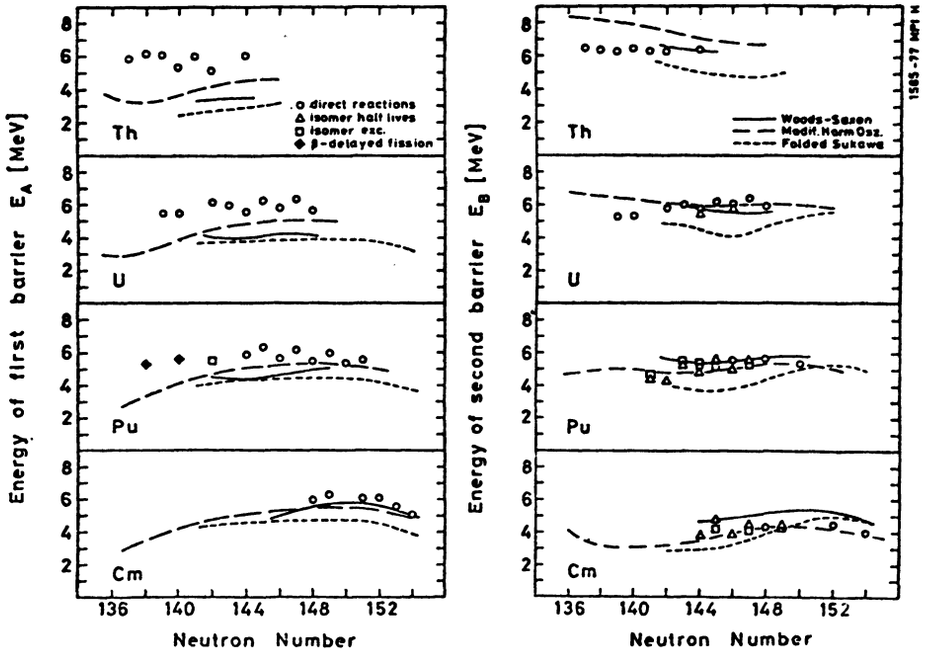

Fig. 5.5

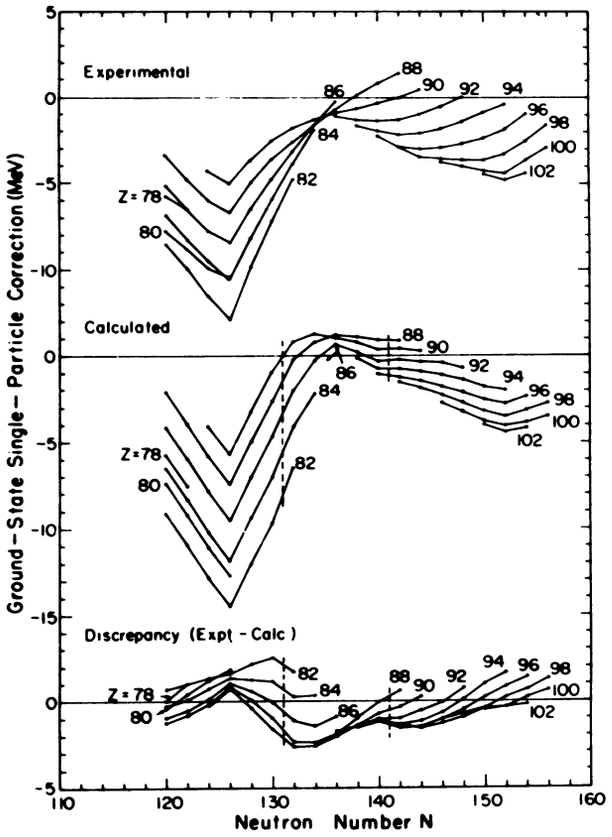

Fig. 5.6

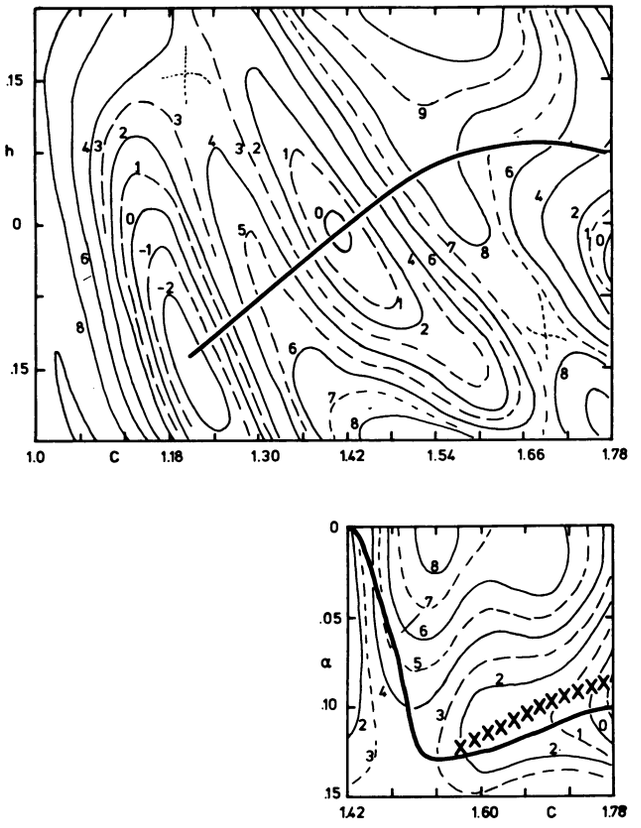

Fig. 5.7

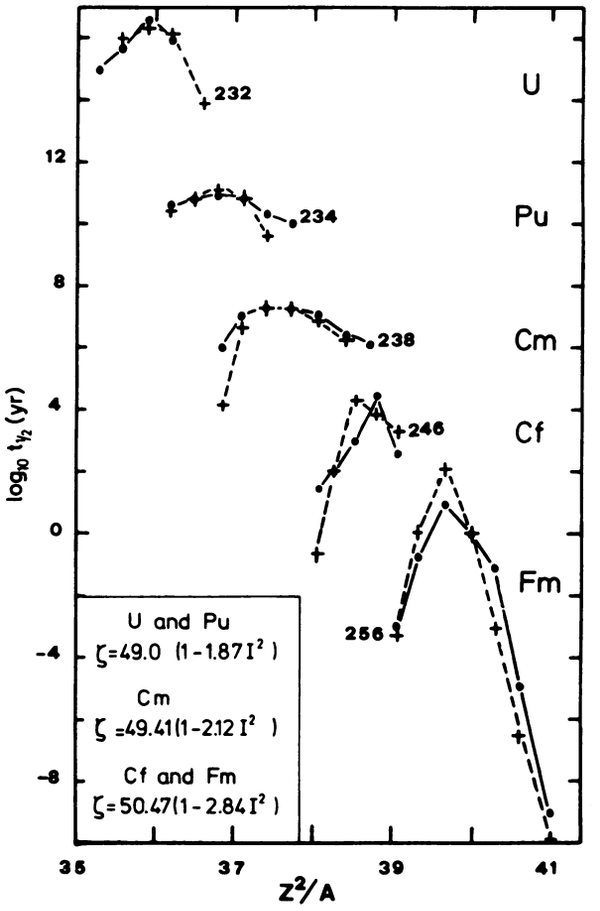

Fig. 5.8